Check for updates

Review of discrete fracture network characterization for geothermal energy extraction

Giacomo Medici[1]*, Fanlin Ling[2] and Junlong Shang[2]

[1]Dipartimento di Scienze della Terra, Universita' di Romas "La Sapienza", Roma, Italy, [2]James Watt School of Engineering, University of Glasgow, Glasgow, United Kingdom

Geothermal reservoirs are highly anisotropic and heterogeneous, and thus require a variety of structural geology, geomechanical, remote sensing, geophysical and hydraulic techniques to inform Discrete Fracture Network flow models. Following the Paris Agreement on reduction of carbon emissions, such reservoirs have received more attention and new techniques that support Discrete Fracture Network models were developed. A comprehensive review is therefore needed to merge innovative and traditional technical approaches into a coherent framework to enhance the extraction of geothermal energy from the deep subsurface. Traditionally, statistics extracted from structural scanlines and unmanned aerial vehicle surveys on analogues represent optimum ways to constrain the length of joints, bedding planes, and faults, thereby generating a model of the network of fractures. Combining borehole images with seismic attributes has also proven to be an excellent approach that supports the stochastic generation of Discrete Fracture Network models by detecting the orientation, density, and dominant trends of the fractures in the reservoirs. However, to move forward to flow modelling, computation of transmissivities from pumping tests, and the determination of hydraulically active fractures allow the computation of the hydraulic aperture in permeable sedimentary rocks. The latter parameter is fundamental to simulating flow in a network of discrete fractures. The mechanical aperture can also be estimated based on the characterization of geomechanical parameters (Poisson's ratio, and Young's modulus) in Hot Dry Rocks of igneous-metamorphic origin. Compared with previous review studies, this paper will be the first to describe all the geological and hydro-geophysical techniques that inform Discrete Fracture Network development in geothermal frameworks. We therefore envisage that this paper represents a useful and holistic guide for future projects on preparing DFN models.

KEYWORDS

geothermal reservoirs, discrete fractures, geophysics, hydraulic data, structural geology

1 Introduction

The exponential advances in geo-modelling of the last 30 years have yielded new approaches for representing fluid flow in the aquifers that are exploited for drinkable water, conventional oil and gas, shale gas and geothermal reservoirs of both hydrothermal and Hot Dry Rock (HDR) nature (Bigi et al., 2013; Hartmann et al., 2014; Przybycin et al., 2017; Lancia et al., 2018; Doran et al., 2021; Dorhjie et al., 2022; Hering et al., 2023; Medici and West, 2023; Melouah et al., 2023). Many researchers have pointed out that these advances in modelling have not been followed by adequate attention to the experimental and technical components that are necessary to represent the complexity of porous and fractured
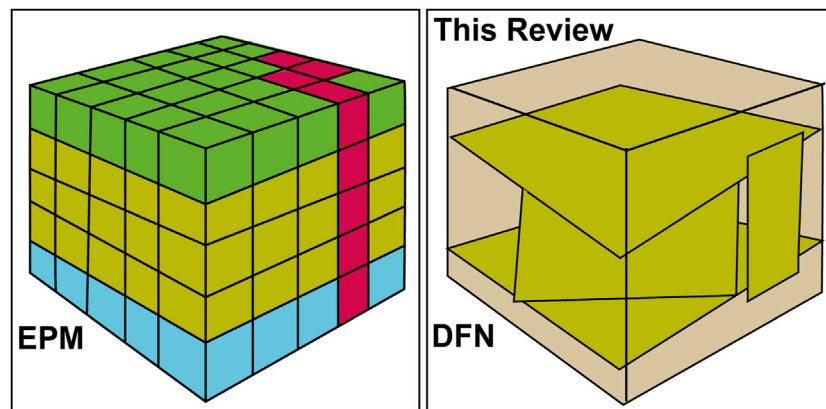
FIGURE 1
EPM vs. DFN modelling in low, medium and high enthalpy geothermal energy.

geological media (Aydin, 2000; Frosch et al., 2000; Kristensen et al., 2016; Colombera et al., 2019). However, in the last 5 years, some new structural (LiDAR scan tests, and UAV surveys) and geophysical (Ultra Sonic Borehole Imager, Active Line Source temperature logging, and fibre optic sensing for fluid temperature) techniques have been developed to inform the discrete fracture network (DFN) flow models used in the production of geothermal energy (e.g., Aabø et al., 2005; Lima et al., 2019; Tavani et al., 2022; Welch, 2023). This renewed interest has occurred to meet the ambitious targets set by the Paris Agreement. According to this agreement, the reduction of greenhouse gas emission is imperative, and it can be reduced by the decarbonisation of our energy grid. In their attempts to reduce such emissions, researchers have recognized the importance of geothermal resources, which are essential in view of their direct application to sustainable heating and electricity production (Rubio-Maya et al., 2015; Salazar et al., 2017; Ciapala et al., 2021; Rybach, 2022).

As a consequence of the exigencies of a sustainable society, a review of the techniques necessary to generate robust flow models in geothermal reservoirs is needed to (i) approximate the anisotropic and heterogeneous nature of geological media, (ii) account for the exponential proliferation of numerical solutions in the last 30 years, and (iii) integrate established and new experimental approaches. The most recent technical approaches incorporate the use of UAV surveys/LiDAR tablets in the field of remote sensing and seismic attributes from the field of geophysics (Aabø et al., 2005; Smeraglia et al., 2021; Welch et al., 2022). These new techniques also need to be integrated with the more traditional ones (structural scanline surveys, fullbore formation microimager logging, acoustic and optical televiewer logs), for reconstruction of the 3D network of fractures. The techniques mentioned above allow the generation of 3D discrete fractures with more realistic geometry that can be used to characterize geothermal reservoirs. Notably, other traditional methodologies are necessary when the purpose of the modelling is to eventually understand the dynamics of flow. In the latter case, the hydraulic aperture is also fundamental to characterize Discrete Fracture Network (DFN) models (Quinn et al., 2020; Romano et al., 2020; Hale et al., 2021).

To determine the applicability of the techniques reviewed in this paper, models of fluid flow in a DFN framework are necessary

for medium (fluid temperature ranging from 90°C to 150°C) and high enthalpy (fluid temperature equal or higher than 150°C) hydrothermal reservoirs for fractured rocks of sedimentary nature (see conceptual scheme in Figure 1). Here, such geothermal resources are buried in the depth range of approximately 0.15–5.0 km (Busby, 2014; Medici et al., 2019a; De Franco et al., 2019; Melouah et al., 2021a; Melouah et al., 2021b; Zheng et al., 2021; Xu et al., 2022; Zuo et al., 2022; Eldosouky et al., 2023). In this depth range, the permeability of the rocks is relatively low due to processes of groundwater dissolution which are minimal, and DFN is needed to unravel the amount of heat that can be extracted, and economically feasible by studying the rock mass at a scale small enough (cubes of 0–3 km of length) (Müller et al., 2010; Medici et al., 2018). The DFN approach (Figure 1) is also fundamental in Enhanced Geothermal Systems (EGS) to produce geothermal fluids from igneous and metamorphic HDR that are characterized by particularly low permeability due to a reduced hydraulic connectivity of the natural fracturing network (Lu et al., 2023). In this framework, fluids are injected at a pressure that could reactivate pre-existing fractures or create new ones. EGS allows to (i) rise the fracture connectivity and hence the permeability of the reservoir, and (ii) increase the flow-surface contacts to favour heat exchange between rock and injected fluid (Breede et al., 2013; Kong et al., 2014; Jain et al., 2015; Wu and Li, 2020). By contrast, the Equivalent Porous Medium (EPM) is more commonly used to model flow and heating at much shallower depths to manage low-enthalpy geothermal resources (Figure 1). EPM models can be used to model transfer of heat plumes. Such EPM models allow reproducing both the conductive and advective heat transport by groundwater in the shallow subsurface for the planning of heat pumps (García-Gil et al., 2020; Abesser et al., 2021). EPM and DFN approaches shown in Figure 1 can also be used in the same geothermal project. In fact, in a variety of EGS projects, a DFN is used to estimate the permeability in three dimensions by defining the tensor. Then, this information on the permeability tensor can be transferred to EPM models that will be anisotropic for flow applications in geothermal reservoirs of medium and high enthalpy nature (Janiga et al., 2022; Ma et al., 2022).
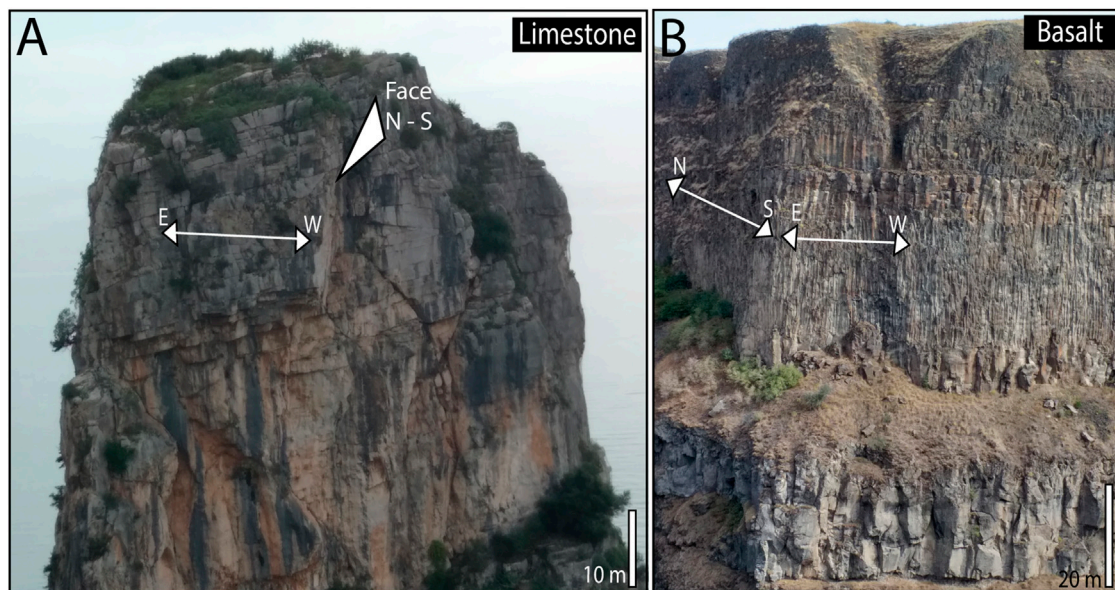
FIGURE 2
Outcrop exposures of fractured rocks at cliffs. **(A)** Cretaceous Limestone on the Tyrrhenian Sea in southern Latium, Italy, **(B)** Miocene volcanic rocks of the Columbia River Basalt Group at the Palouse Falls, Washington, United States.

Some of the techniques described in this research to inform DFN models are common to the rock mechanics sector due to the importance of rock discontinuities on the stability of rock engineering infrastructures (Shang et al., 2016; Schilirò et al., 2022), the excavation of rock caverns for the storage of liquefied natural gas (Xiao et al., 2019), and the mining and oilandgas sectors where fractures play a role in the extraction of fluids (Bauer and Tóth, 2017). Therefore, this review is primarily addressed to a public of experts in geothermal energy, although a wider range of geoscientists may also find it of interest.

A look at recent literature that summarizes current knowledge of DFN with a focus on geothermal resources reveals a special issue (Mazzoli, 2022) with nine contributions that examine the link between structural geology and extraction of fluids. All nine contributions describe the tectonic structures of reservoir analogues (Filipovich et al., 2020; Bossennec et al., 2022; Dragoni and Santini, 2022), the fluid-rock interaction (Liotta et al., 2021; Gudmundsson, 2022), and heat flow computing and mapping (Santini et al., 2020; 2021; Majorowicz, 2021; Majorowicz and Grasby, 2021). Previous reviews in the field of geothermal energy have focused on the exploration of specific regions characterized by elevated geothermal gradients (e.g., Minissale, 1991; Breede et al., 2013; Manzella et al., 2018; Majorowicz, 2021). Other attempts to review the literature on geothermics have focused on numerical modelling of single and dual porosity systems, and description of machine learning techniques (Hayashi et al., 1999; Axelsson, 2010; Okoroafor et al., 2022) or combining different approaches to flow modelling (discrete fracture network, equivalent porous medium, and conduit) in specific lithologies (Selroos et al., 2002; Medici et al., 2021). By contrast, this review will be the first one to describe exclusively technological and experimental techniques that inform DFN in geothermal frameworks in a variety of lithologies with cut-off to the end of the year 2023 (Figures 2, 3).

In summary, analysing structural, remote sensing, geomechanical, hydro-geophysical methods, this review provides guidelines for defining the physical parameters used to inform DFN flow models of geothermal reservoirs discerning advantages/limitations and conditions of application of the methods. Specific research objectives are to provide descriptions of: (i) scanline and Unmanned Aerial Vehicles surveys to determine orientation, density, and length of fractures, (ii) combinations of Acoustic Televiewer logging and seismic attributes to guide stochastic generation of a DFN, (iii) hydro-geophysical techniques for determination of hydraulically active fractures and hydraulic apertures, and (iv) collection of geomechanical parameters for generation of a DFN.

2 Fracture network characterization

2.1 Scanline survey

Scanline surveys are used to characterise the network of rock discontinuities in outcrops (e.g., road cuts, quarries) that represent an analogue of the reservoir. The geometries of the fractures are measured in outcrop assuming a tectonic history sufficiently similar to enable comparison in terms of fracture density and persistence (Bauer et al., 2017). The methodology consists of recording dip angle and direction, position along the line, length, mechanical aperture and tortuosity of the rock discontinuities. The tortuosity is defined as the ratio between the length of the curve and the distance between its ends and is rarely measured by surveyors. Instead, surveyors record this parameter by assigning an index, and therefore the
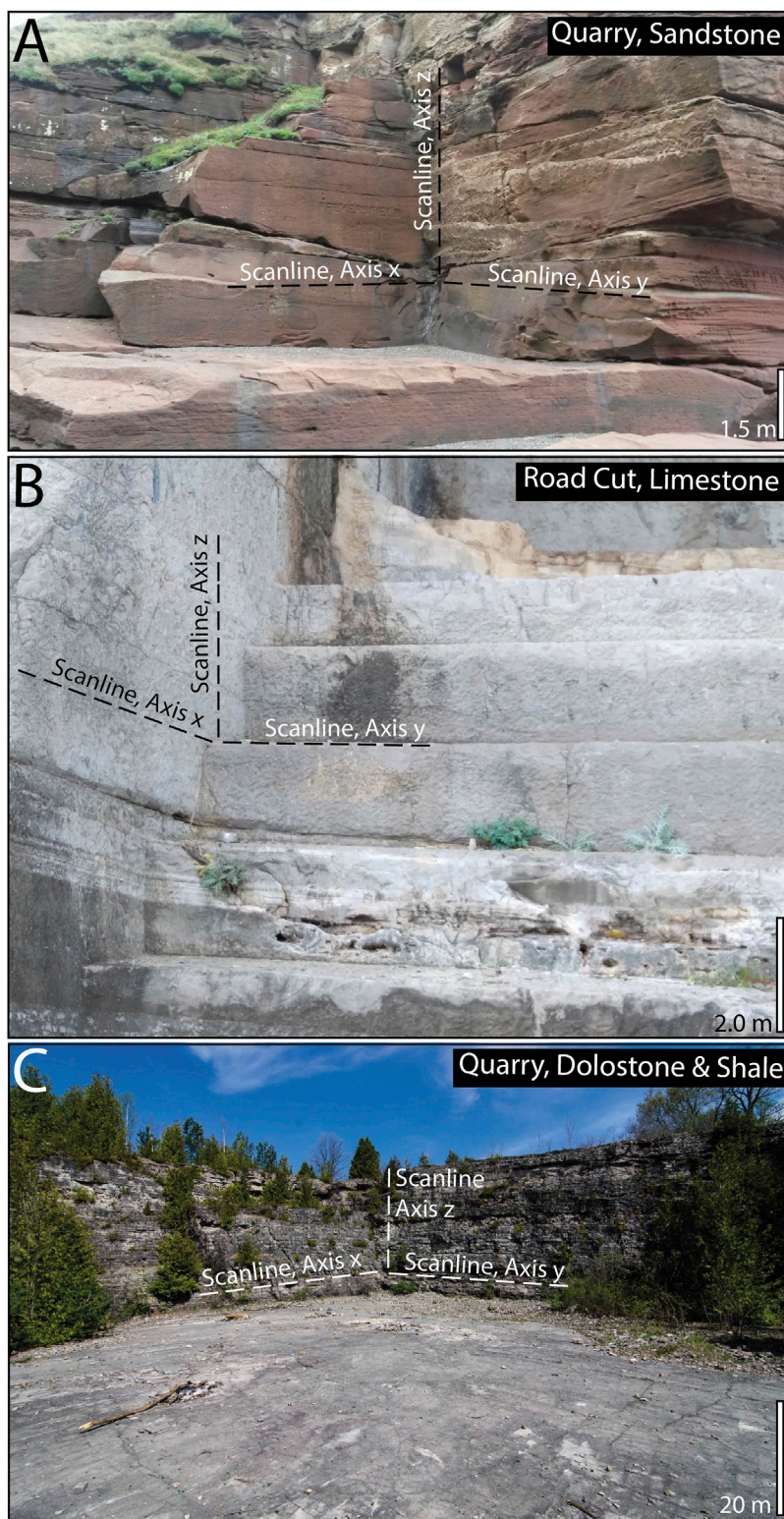
FIGURE 3
Outcrop exposures suitable for scanline surveys along orthogonal axes in different lithologies. **(A)** Triassic Sandstone on a disused quarry at the Fleswick Bay in NW England, **(B)** Cretaceous Limestone at Terracina in Central Italy along a road cut, and **(C)** Dolostone and shale at the Reformatory Quarry at Guelph, Ontario, Canada.
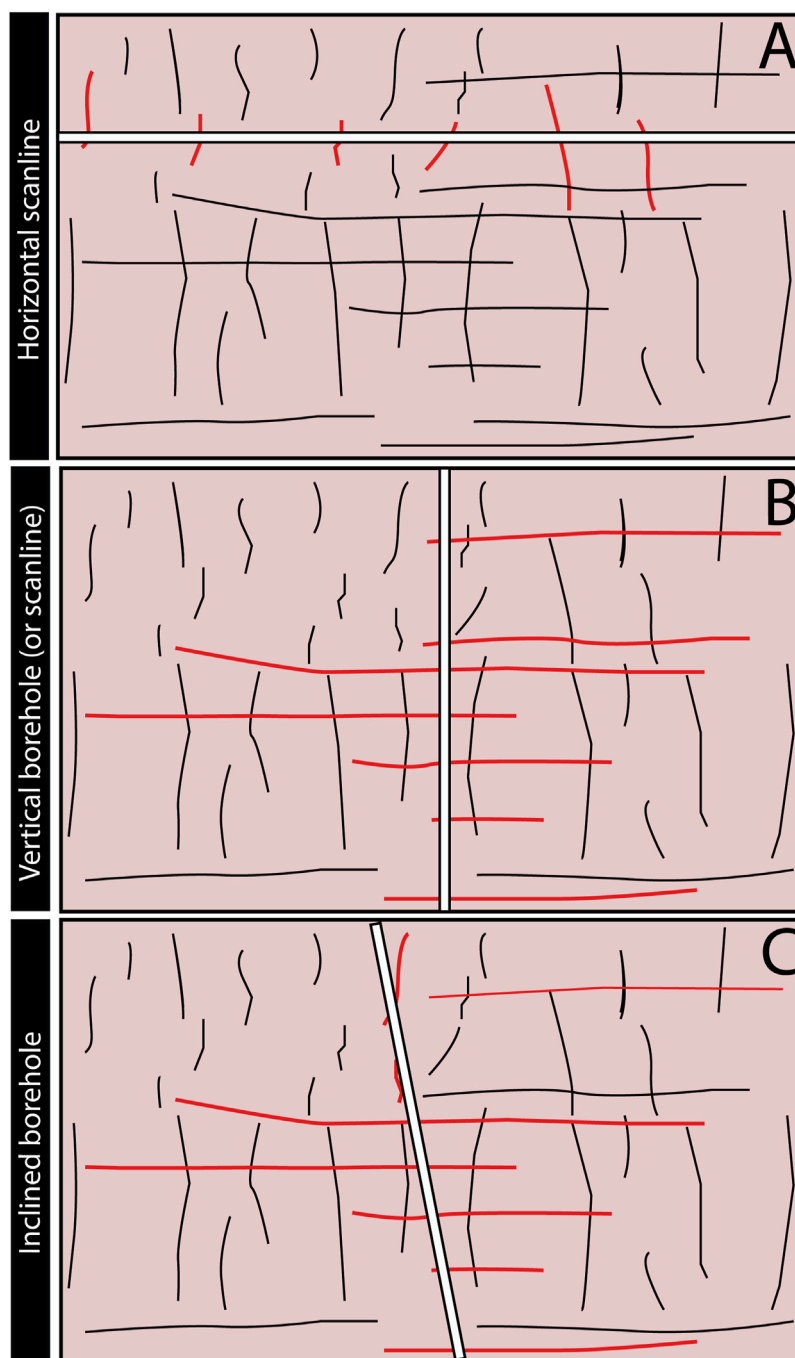
FIGURE 4
Proportion peaked (thick lines) and un-peaked (thin lines) fractures as function of the methodology and the orientation of the borehole or scanline.
(A) sub-horizontal scanlines, **(B)** vertical boreholes or scanlines, and **(C)** inclined borehole.

measurement is semi-quantitative (Tsang, 1984; Hitchmough et al., 2007).

Using scanline surveys to determine geometrical characteristics of joints, fractures, stylolites and bedding plane discontinuities has many advantages (Billi et al., 2003; Lemieux et al., 2009; Lancia et al., 2020). Firstly, by performing the survey on orthogonal rock walls measurements can be performed in the three dimentions (two horizontal lines, and one vertical) which match fracture network models that incorporate the third spatial axis. The performance of a single horizontal scanline on a vertical face may fail to detect small size discontinuities or those that are roughly parallel to the scanline or concealed, resulting in bias during sampling (Shang et al., 2018). To avoid bias, the condition of having orthogonal walls is commonly chosen at quarries (Figures 3A–C), and under this condition the majority of literature on this specific topic has been produced (e.g., Wealthall et al., 2001; Hitchmough et al., 2007; Lemieux et al., 2009; Agosta et al., 2010; Medici et al., 2016). Secondly, the potential to record parameters along both vertical, and horizontal lines reduces

FIGURE 5
UAV survey to extract fracture statistics on the pavement of fractured dolostone at Guelph, Ontario, Canada.

or eliminates bias by sampling discontinuities that are characterized by a range of dipping angles (see conceptual scheme in Figures 4A, B). Thirdly, this methodology allows the measurement of the length of the rock discontinuities that cannot be measured directly in boreholes (Aydin, 2000; Bauer et al., 2017; Lepillier et al., 2019; 2020).

However, scanline surveys that are performed to represent the fracture network of geothermal reservoirs have some limitations. The mechanical aperture does not fit the aperture of the reservoirs. This issue occurs for the enhancement of the aperture due to an unconfined free face at quarries and road cuts (Kana et al., 2013). Weathering can also enlarge the mechanical aperture. The lithostatic load is much higher in reservoirs buried at depths between 0.5 and 5 km. The tectonic history of outcropping rock can differ from the same rock buried in the subsurface, therefore the outcropping rock might show a different pattern of rock discontinuities (Aydin, 2000; Guerriero et al., 2011; Vitale et al., 2012). Scanline surveys are also characterized by a degree of subjectivity. Indeed, surveyors that performed a scanline in the same position multiple times produced each time different results (Hitchmough et al., 2007).

Of note, some authors have introduced a simplified approach named "fast scanline" that exclusively incorporates information on dip angle and direction, and position along the line, thereby reducing the scan time (Carminati et al., 2014). This fast approach should be discarded for scanline surveys used to reconstruct of the three dimensional pattern of rock discontinuities. The length of rock discontinuities is a fundamental parameter that must be recorded in an outcrop in a DFN research project. By contrast, neglecting the mechanical aperture may be acceptable due to the non representativity of that parameter in the outcrop (Bauer et al., 2017). The tortuosity can also be neglected by choosing to build DFN flow models in three dimensions with tabular discontinuities.

Dip angle and directions, position and length of the fracture can also be extrapolated from LiDAR scan tests using tablets in the field (Apple iPAD, iPAD Pro and iPhone 12 Pro). This method is faster than traditional scanline tests and provide accurate geometrical data (Tavani et al., 2022; Allmendinger and Karabinos, 2023). However, the limitation of technologically scanning an outcrop without measuring each rock discontinuity consists on loosing detail on recognizing geological nature (e.g., bedding planes vs. stylolites).

2.2 Unmanned aerial vehicle

In practice, substantial parts of rock outcrops are not accessible for structural scanlines. To sidestep this issue, unmanned aerial vehicles (UAV; Figure 5) are used to acquire information on the geometries of the fractures at cliffs such as those shown in Figure 2, where surveyors either cannot walk or transport equipment on top. UAVs are characterized by their megapixel photosensors, and are therefore capable of collecting numerous ($\sim 10^2$–10^3) photos of the outcrop with a certain percentage (e.g., 70%) of spatial overlap. After the photos have been taken, the next step is to extract information on the geometry of rock discontinuities by manual digitalization of joints, bedding planes, and faults (Binda et al., 2021). The UAV for applications in geosciences are characterized by different airframes polystyrene, plastic, aluminum, and carbon fiber for the most modern (Giordan et al., 2020). All the rock discontinuities are rigorously georeferenced, and the described approach allows for the collection of information on dip angle and direction, and the density of fractures. This information is equivalent to data obtained from structural scanlines acquired in road cuts and quarries. Consequently, the statistics on the fracturing network obtained from structural scanlines and from UAV can be integrated as proposed by Smeraglia et al. (2021). These authors combined information from scanline surveys on road cuts with fracture statistics from UAV photos of the unaccessible portion of a cliff that is characterized by Cretaceous limestones. The information

acquired by combining structural surveys on road cuts and UAV photogrammetry was used to generate DFN models of faulted and host-rock blocks using the MOVE Software Suite. Using the same suite, DFN models of fractured Mesozoic limestones in southern Italy were generated by Giuffrida et al. (2020), combining structural analysis in the field with the extraction of geometrical fracture data from an UAV as the one shown in Figure 5.

Furthermore, statistics on fracture geometry extracted using UAV has been recently used by a variety of authors on different lithologies. Francioni et al. (2020) extracted fracture statistics from a UAV survey to generate a 3D DFN model of marls and limestone of the Jurassic Age in the Abruzzi region in the area of Scanno Lake. A DFN model in three dimensions has also been generated using a UAV survey in the Triassic granites of the Gonghe Basin in China in the framework of a high enthalpy geothermal project for the development of an EGS system (Zhang B. et al., 2022).

UAV surveys for the generation of 3D DFN models have also been used on the Cretaceous limestones of the Sorrento Peninsula in southern Italy (Schilirò et al., 2022), the Jurassic marble of the Apuan Alps in central-western Italy (Salvini et al., 2017), the Cretaceous sandstone in northern Togo (Akara et al., 2020), and the Triassic sandstone near Sydney in Australia (Tuckey, 2022). Of note, UAV surveys similarly to LiDAR tablets show a limitation on discerning the geological nature of the rock discontinuity.

2.3 Borehole images

Optical (OTV), Acoustic televiewer (ATV) and Fullbore formation microimager (FMI) images show continuous views of the borehole wall, and allow to record dip direction and angle, and position along the borehole in fractured rocks. Dip direction and angle can be determined by structure peaking after acquisition and processing of the dataset (Williams and Johnson, 2004). The position of the rock discontinuities along the borehole allows determining the fracturing intensity that is a required parameter to build DFN models in three dimensions (Guo et al., 2022; Xiao and He, 2022).

Notably, OTV and ATV logs provide the same information, although differences have been detected by applying the two methods. Fractures are more clearly defined under a wider range of conditions on ATV images than on OTV images including dark-coloured rocks, cloudy borehole water, and coated borehole walls. Hence, the most important dataset to build DFN models is the one from ATV. A high resolution example of ATV is the Schlumberger Ultra Sonic Borehole Imager (UBI) that is commonly used in medium and high enthalpy geothermal systems. This type of ATV is characterized by an azimuthal resolution of $2°$, vertical resolution from $0.2'$ to $1.0'$ depending on the pulse frequency (Genter et al., 1997; Gaillot et al., 2007). However, OTV images allow for the direct viewing of the type of fracture, and relation between lithology, fractures, foliation, and bedding (Williams and Johnson, 2004; Medici et al., 2016; Medici et al., 2019b). Therefore, the most powerful approach is the combined application of imaging, by using ATV to determine the orientation of the fractures and OTV to interpret its nature (e.g., distinguish a stylolite from an open bedding plane fracture). The FMI tool is also used in geothermal fields to determine the orientation of the fractures. This wireline tool works by emitting a focused current from the four pads of the logging tool into the geological formations. The intensity variations of the electrical resistivity

are measured and provide an image of the rock walls. The FMI provide the same output of OTV and ATV logs, but it is preferred in water based mud wells that can occur in fluivial and turbidite deposits (Bauer et al., 2017).

The principal advantage of OTV, ATV, and FMI logs with respect to traditional scanlines, LiDAR scan tests and UAV surveys is the opportunity to acquire the dataset directly in the geothermal reservoir. The ATV log also provides the value of mechanical aperture due to the fact that open discontinuities are characterized by low amplitude and travel times of the acoustic waves. However, the aperture highlighted by the acoustic televiewer is much higher than the real hydraulic aperture (the necessary parameter for DFN flow models) as demonstrated by Maldaner et al. (2018) in a Silurian fractured aquifer of carbonate origin in Ontario.

Data on the fracturing intensity are affected by bias especially when only vertical wells are used in the geothermal projects (Terzaghi, 1965; Lato et al., 2010; Andrews et al., 2019). In fact, vertical wells tend to pick low ($0°$–$30°$) angle discontinuities if the stratigraphy is characterized by sub-horizontal beds as illustrated in Figure 4A. To address this issue, the presence of inclined (or deviated) wells with a plunge of $60°$ from horizontal allows picking a higher proportion of sub-vertical joints (Figure 4C; Munn et al., 2020). The inclined boreholes have on average, a 20% proportion of sub-vertical ($50°$–$90°$). This proportion is lower, 6% by arithmetic average, in the vertical boreholes that are biased towards the sub-horizontal discontinuities (Figure 4A). Therefore, the presence of vertical and inclined wells provide more robust statistics on fracturing intensity to build Discrete Fracture Network (DFN) models.

2.4 Seismic attributes

The use of seismic attributes is used to generated 3D DFN models due to their capability to detect the principal trends, and presence of faults that can represent preferential flow pathways for the geothermal fluids (Bense et al., 2013; 2016; Schneider et al., 2016; Cho et al., 2019; Marchesini et al., 2019; Cho, 2021; Fadel et al., 2022; Huang et al., 2022; Xing et al., 2022; Zhang E. Y. et al., 2022; Chiodini et al., 2023).

An integrative workflow to the characterization of the 3D network of fractures have been recently developed in the Cretaceous Danish Chalk in the North Sea (Aabø et al., 2005; Aabø et al., 2023; Smith and Welch, 2023). This approach is based on reservoir data from ATV borehole images, cores and seismic attributes (Aabø et al., 2005). ATV and core data provide information on fracture orientation from a variety of wells. Seismic attributes are capable to detect the principal trends of fractures and faults of the reservoirs. The scale-gap between the data sets is bridged by the introduction of two antracked attribute volumes, which display structural trends below the resolution of amplitude seismic. Further insight into the geometries of subsurface fracture systems is obtained from fracture density logs from ATV/OTV/FMI and cores, which provide an opportunity to study spatial distribution of fractures as well as a qualitative measure of fracture clustering. Cumulative density distribution plots and calculation of the variation coefficient of fracture spacing provide a more quantitative analysis of the fracture distribution (Aabø et al.,
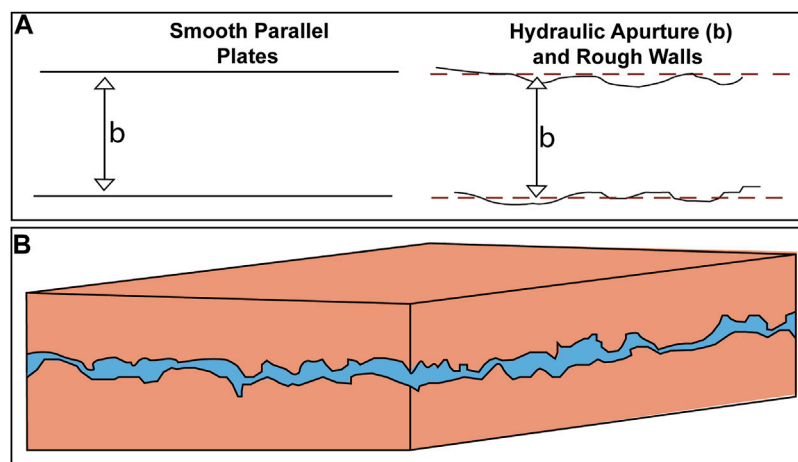
FIGURE 6
Hydraulic aperture in fractured rocks. **(A)** Smooth parallel plate vs. rough walled models, and **(B)** real mechanical aperture.

2005). These results have served as inputs into discrete fracture network models that have been then stochastically generated using the new DFN Generator v2.0 now available as a plugin in Petrel (Welch et al., 2022; Welch, 2023).

3 Hydraulic characterization

3.1 Cubic law

DFN models that are used to simulate flow require input values from fracture intensity, length and orientation from outcrop and borehole image (ATV, OTV, and FMI) logs and the apertures of the rock discontinuities. The latter parameter, which represents the aperture of a parallel walled fracture, is the most important parameter when simulating flow in a DFN framework, and is directly proportional to the permeability of the rocks. Indeed, highly permeable rocks are characterized by an elevated number of fractures with large hydraulic aperture (Oron and Berkowitz, 1998; Dijk et al., 1999; Berkowitz, 2002). The hydraulic aperture (see conceptual scheme in Figure 6A) is assumed to be a smoothed parallel plate in DFN flow modelling in a variety of numerical codes such as dfnWorks, TOUGH2, MAFIC, and PFLOTRAN (Zhang and Yin, 2014; Hyman et al., 2015; Ji and Koh, 2017; Romano et al., 2020). This assumption is related to the fact that two straight lines represent the lower and upper bounds of the modelled fracture. The straight lines average the peaks and valleys of rough real walls of joints and bedding plane fractures (Figures 6A, B; Renshaw, 1995). Hence, given this assumption, the hydraulic aperture (b) is expressed by Eq. 1 based on the implementation of the cubic law assuming a laminar flow (Romm, 1966).

$$b = \sqrt[3]{\frac{12\nu T}{gN}} \qquad (1)$$

where T is the screened interval transmissivity, g is the gravitational acceleration, ν the kinematic viscosity of hot water in the geothermal reservoir, and N the number of flowing fractures intersecting the

screened interval. Screened interval transmissivity (T) is determined by a well test, and is the product of the rock hydraulic conductivity and the packer screen length. Given the fact that there is no need to experimentally determine g and ν, geophysically determining "b" means characterizing the transmissivity of the fractured rock using well tests, and detecting the number of hydraulically active fractures using either standard fluid logging or more advanced techniques (Romm, 1966; Haffen et al., 2013). In a DFN framework for geothermal energy production, all the rock discontinuities need to be represented in the 3D domain even though not all of them are hydraulically active. In fact, inactive fractures can represent either boundaries that can influence the flow, or surfaces of mechanical weakness that play a role in the development of EGS systems of igneous and metamorphic origin (Caulk and Tomac, 2017; Förster et al., 2018; Freitag et al., 2022). Reliable models of 3D networks of fractures are fundamental in EGS systems to predict the new framework of rock discontinuities after the injecting of fluids at high pressure. This engineering process changes the pre-existing fractures by enhancing their (i) length, (ii) degree of connectivity, (iii) transmissivity, and (iv) storativity as geothermal reservoirs (Lepillier et al., 2019; Abe and Horne, 2023).

3.2 Well tests

A variety of well tests are used to determine the transmissivity of deep saline aquifers that host medium and high enthalpy geothermal resources in lithified sedimentary rocks. Boreholes are typically characterized by multiple packers in deep (~0.15–~2.0 km) saline aquifers, and the Westbay technologies proposed by Schlumberger can be used at such elevated depths in hydrothermal reservoirs (Streetly et al., 2000; Streetly et al., 2006; Senel et al., 2014; Streetly and Heathcote, 2018).

Constant flow rate pumping tests provides T by analysing the drawdown, which is a fundamental parameter in the determination of the hydraulic aperture using Eq. 1. The recovery phase (flow rate equal to zero after shutting off the pump) can also provide an

estimate of T that should approximate the result of the drawdown in a reliable test (Hantush, 1966; Saleem, 1970; Medici et al., 2016). Additionally, constant head step tests accurately identify the extent of the Darcian flow and are also used to determine T by analysing the drawdown. Therefore, "b" can be extrapolated by analysing the drowdown. Such tests are characterized by raising the flow rate in at least four steps, before shutting off the pump (Clark, 1977; Birsoy and Summers, 1980; Kawecki, 1995; Lennox, 1996). The T value from the step test analysis can also be crossed with the T value from the recovery. Additionally, in this case, reliable tests are characterized by very similar T values from the drawdown step and the recovery phase. Notably, T values from the recovery phase neglect the well loss correction, and can therefore be 20% lower than T values obtained from the more reliable step recovery analysis (Eden and Hazel, 1973; Clark, 1977; Mathias and Todman, 2010). A correction that accounts for the density changes due to the temperatures, and viscosities of geothermal fluids has recently been proposed to determine transmissivity from constant flow rate, recovery and step tests (Klinka and Gutierrez, 2020). The correction arises from the fact that traditional methods for analysis of pumping tests (e.g., Hantush, 1966; Eden and Hazel, 1973; Clark, 1977; Birsoy and Summers, 1980) are suitable in shallow aquifers which are characterized by lower temperatures and different density with respect to geothermal fluids.

3.3 Borehole geophysical logging for fluids

Borehole geophysical logging techniques are used to determine the number of hydraulically active fractures (N) in a packer interval to determine the hydraulic aperture using Eq. 1, which is derived using the cubic law (Romm, 1966). The most common approach is to combine fluid temperature, electrical conductivity and velocity logs to detect either inflow or outflow points using flow meters (Hicks and Berry, 1956; Paillet and Pedler, 1996; Paillet et al., 2002; Bixley et al., 2009; Massiot et al., 2015; Wight and Bennett, 2015; Blöcher et al., 2016). By crossing this information with optical and acoustic televiewer images that show the fractures at flowing points the number (N in Eq. 1) of hydraulically active rock discontinuities that enable fluid flow is determined. The transmissivity is known from well tests performed in Westbay packers that are located at different depths. Hence, the hydraulic aperture is determined by using Eq. 1 at a variety of depths in the subsurface, and DFN flow models can be rigorously informed.

A more innovative approach that can be used to determine the number of hydraulically active fractures in deep saline aquifers is Active Line Source (ALS) temperature logging. The ALS temperature logging data from inside a FLUTe™ lined borehole must be collected and processed as described by Pehme et al. (2013) to generate thermal deviation logs where each aberration in the deviation log represents a change in temperature that suggests a fracture with active flow. After the addition of heat along a cable deployed into the static water column inside the liner, a high-resolution temperature probe with a specific resolution of 10^{-4}°C is used to measure temperature variability. The ALS temperature logging method is considered a qualitative log that identifies very small temperature deviations that have been shown to correspond to active flow (Pehme et al., 2007; 2013). This methodology is highly

sensitive, and capable of detecting all the flowing fractures needed to determine N, and therefore the hydraulic aperture using the derivation of the cubic law expressed in Eq. 1. Fibre optic sensing-based solutions produced by Silixa are also suitable for temperature monitoring and detection of the number (N) of hydraulically active fractures in geothermal reservoirs (Stork et al., 2020).

Aside from the technology used for detection of hydraulically active rock discontinuities, a percentage (approximately 100%) of flowing fractures characterize the geothermal reservoirs of igneous and metamorphic origin under pumped conditions. These types of rocks show a low permeability intergranular porosity in the unfractured blocks (Szanyi, J. and Kovács, B., 2010; Randolph and Saar, 2011; Agemar et al., 2014; Medici et al., 2018). In the latter case, the hydraulic conductivity of the intergranular pores can be neglected in DFN (single permeability geothermal reservoirs), but all the fractures of the network are active and need to be included in the flow model. In contrast, geothermal reservoirs of sedimentary origin (e.g., porous carbonates, not tight sandstone) are characterized by a relatively permeable matrix (dual permeability geothermal reservoirs), and the percentage of hydraulically active fractures range from 20% to 80% of the total under pumped conditions (Tellam and Barker, 2006; Quinn et al., 2015; Goupil et al., 2022). Therefore, the permeability of the matrix blocks should not be neglected in the latter case by embedding the discrete fractures in a porous matrix. The permeability of the matrix can be measured in the laboratory by using a mini-permeameter to test rock samples from cores (Shafiq and Mahmud, 2017; Cant et al., 2018; Bohnsack et al., 2020; Fazio et al., 2021).

4 Geomechanical characterization

Collection of geomechanical parameters is also needed to build DFN models in EGS systems in igneous and metamorphic rocks. Uniaxial Compressive Strength, Poisson's ratio, and Young's modulus need to be determined in the laboratory by using either analogous outcropping rocks, or core samples (Bozzano et al., 2012; Torabi et al., 2018; Shang, 2020; Fiorucci et al., 2020; Marmoni et al., 2020). Of note, outcropping rocks provide different Uniaxial Compressive Strength and Young's modulus values respect to the same geological formations cored from the geothermal reservoir. The discrepancy can be up to 50%; the samples from the outcrop are mechanically weaker than those of the reservoir due to the weathering effects on cliffs, quarry walls and road cuts (Bauer et al., 2017). The above mentioned mechanical parameters (compressive strength, Young's modulus, and Poisson's ratio) ideally need to be determined using triaxial compressive tests. These mechanical tests are characterized by lateral confinement and a longer duration than uniaxial tests. Such conditions induce the samples to be either more ductile or closer of the mechanical behaviour of the subsurface under triaxial forces (Mogi, 1971; Li et al., 1999; Sari and Karpuz, 2006).

The most reliable approach to the geomechanical characterization of a geothermal reservoir is therefore characterize compressive strength, Young's Modulus and Poisson's ratio running mechanical tests with lateral confinement of samples cored from the reservoir. These geomechanical

TABLE 1 Summary of the techniques used for construction of the fracturing network with information of the object characterized, depth of investigation and the spatial scale.

Methodology	Object characterized	Depth of investigation (m)	Observation scale (m)
Scanlines	Analogue	0	Outcrop ($\sim10^{0}$–10^{2})
UAV	Analogue	0	Outcrop ($\sim10^{0}$–10^{2})
FMI/ATV/OTV immages	Reservoir	0–5,000	Borehole ($\sim10^{-2}$–10^{-1})
Seismic attributes	Reservoir	0–5,000	Reservoir ($\sim10^{2}$–10^{3})

parameters must be determined on both intact and fractured samples. An intensively fractured geothermal reservoir is assumed being characterized by geomechanical parameters closer to the fissured samples selected from the core cuts (Villeneuve et al., 2018; Rosberg and Erlström, 2021; Freitag et al., 2022).

Determining representative Young's Modulus and Poisson's ratio values for an high enthalpy reservoir is fundamental to estimate the mechanical aperture as function of the stress field under natural conditions. Following this geomechanical approach, the hydraulic aperture is also function of the orientation of the fractures with respect to the principal stress tensor, σ_1. Indeed, more elevated angles between the direction of the σ_1 and the fractures provide lower values of mechanical apertures due to interplays of dilatational and shear forces (Bisdom et al., 2016; 2017). This information on the mechanical aperture need to inform DFN models (Romano et al., 2020; Rosberg and Erlström, 2021; Freitag et al., 2022). Recent and promising research focuses on determining the Young's modulus value directly from the reservoir studying the acoustic impedance from ATV logs; this approach is either alternative or integrative to geomechanical testing in the laboratory of cored samples (Raef et al., 2015; Roshan et al., 2023).

Fractures in DFN models are typically assumed smoothed (Figure 6B), although the roughness can reduce the permeability at least in systems characterized by a low degree of mechanical connectivity (Berkowitz, 2002). Joint Roughness Coefficient (JRC) also needs to be characterized in the laboratory on cored samples to inform DFN models in geothermal reservoirs using laser profilometers (Lee and Ahn, 2004; Młynarczuk, 2010). Alternatively, some authors build DFN models (Figure 1) of geothermal reservoirs reducing the aperture of smoothed fractures that was previously estimated from either hydraulic or geomechanical methods. This correction is not rigorous, but can be a straightforward solution accounting for the roughness of the fractures that reduce either the permeability of the reservoir, or favour heat dispersion in EGS (Fox et al., 2015; Lima et al., 2019; Kittilä et al., 2020a; b).

5 Discussion

5.1 Fracturing network reconstruction

A variety of structural (scanline surveys), remote sensing (UAV), and geophysical (OTV/ATV/FMI images, seismic attributes) methods have been recently developed to generate reliable DFN models (Aabø et al., 2005; Antonellini et al., 2014; Giuffrida et al., 2020). Here, we discuss all together these geological and geophysical techniques for geothermal reservoir characterization. Note that, a summary table

(Table 1) has been proposed to summarize the characteristics of scanline surveys, borehole images, and seismic attributes.

Scanline and UAV surveys have recently been combined to generate DFN models in the outcropping fractured limestone in Central and Southern Italy. These carbonate rocks represent excellent analogues for the geothermal and hydrocarbon reservoirs buried in the subsurface (Giuffrida et al., 2020; Smeraglia et al., 2021). In northern Europe, other researchers propose to combine core data, seismic attributes and acoustic/resistivity images to stochastically generate a DFN afterwards (Aabø et al., 2005; Welch et al., 2022; Smit and Welch, 2023). Of note, once again a holistic approach to a DFN project has been proposed by the geoscience community.

Scanline and UAV surveys of reservoir analogues and the seismic attributes of the effective reservoir make a DFN stochastic generation more reliable. Scanline and UAV surveys provide information on the length of the fractures, and seismic attributes have the unique advantage to bridge the gap between borehole and reservoir scales (Table 1; Salvini et al., 2017; Lepillier et al., 2020; Aabø et al., 2005Aabø et al., 2005; Smeraglia et al., 2021). Acoustic and resistivity image logs acquire data directly from the reservoir (Table 1), and therefore provide the effective orientation of the fractures. Geophysical logging and seismic attributes should be used to determine the orientation of the fracture sets; meanwhile scanline and UAV surveys are needed to determine the length of the principal and secondary sets.

Overall, this paper envisions a future in which researchers combine geophysical techniques, and structural geology surveys in the field to build robust models of the fracturing network. The above described spatial representation of the discrete fractures also supports a rigorous determination of the hydraulic aperture. In fact, this aperture (Figure 6A) depends upon multiple factors including the orientation of the fractures with respect to the stress field tensors σ_1, σ_2, and σ_3 (Bisdom et al., 2016; 2017; Turner et al., 2017; Boersma et al., 2021).

5.2 Hydraulic aperture determination

The ATV logs have also been taken into account by researchers to either determine the Young's modulus of the reservoir rock, or detect the number of hydraulically active fractures in geothermal reservoirs. The latter information needs to be combined with pumping tests in discrete packers to determine the values of the hydraulic apertures that are necessary to move forward to flow modelling (Romano et al., 2020; Medici et al., 2021). Therefore, the efforts in terms of data collection to support flow modelling in a DFN framework also involve ATV/OTV/FMI borehole logging, fluid logging, and pumping tests. Hydraulic
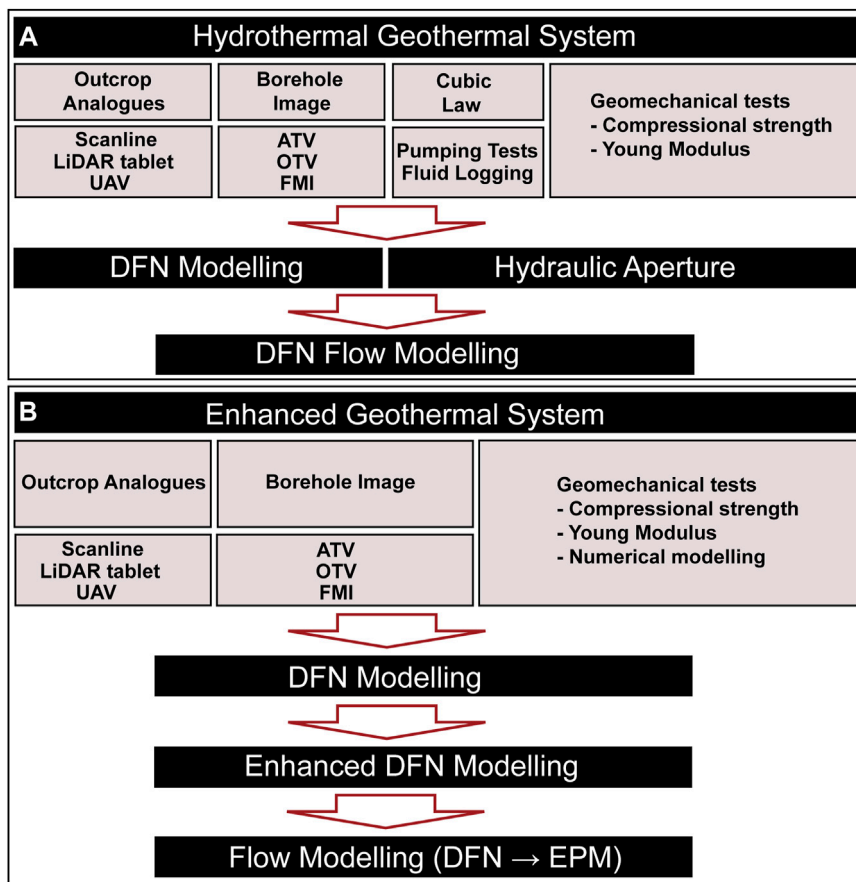
FIGURE 7
Workflows to build a DFN for flow in a geothermal framework. **(A)** Hydrothermal, and **(B)** HDR reservoirs.

testing is more feasible in medium and high enthalpy reservoirs in lithified sedimentary rocks, since such highly layered and fractured rocks tend to be more permeable than igneous and metamorphic lithologies (Clauser, 1992; Younger et al., 2012; Zhang, 2013). The latter two types of rocks characterize EGS-HDR systems; in these geothermal reservoirs, the apertures of the fractures are estimated by the mechanical properties (Poisson's ratio, and Young's modulus), and they vary as functions of the lithostatic load (Bisdom et al., 2016; 2017). This approach arises from the low permeabilities of basement rocks that impede pumping tests during the exploration phase before the injection of fluids to increase the connectivity of the fractures (Abe and Horne, 2023).

Hence, all the described structural, remote sensing, geophysical, geomechanical and hydraulic datasets seem fundamental to generating reliable models of the fracturing network and then moving forward to simulating flow by introducing the hydraulic aperture (Figure 6A). To the authors' knowledge, the techniques described in this review have been combined exclusively in small groups with few components (e.g., outcrop scan lines with fracture statistics from UAV, OTV/ATV/FMI images with seismic attributes, and fluid logging with ATV images). This review therefore points the geothermal community towards a larger combination of the discussed techniques in future E&P projects to optimize recovery of hot

fluids by using DFN to either (i) represent the fracturing network in three dimensions, or (ii) estimate the hydraulic aperture.

5.3 Workflow and future research scenarios

The proposed research has described a variety of geological, geophysical, hydraulic and geomechanical techniques that can be used to investigate geothermal reservoirs at a variety of scales to inform DFN models of permeability and flow. These techniques can be summarized in two workflows for hydrothermal systems (Figure 7A) and enhanced geothermal systems for the extraction from HDR (Figure 7B). The workflows are different because some techniques cannot support extraction of fluids from both types of geothermal systems. Fluid logs and pumping tests cannot be applied to HDR due to the particularly low hydraulic conductivity of igneous and metamorphic rocks at depths (~0.5–2 km) accessed during this investigation (Kittilä et al., 2020a; b). Therefore, the cubic law cannot be applied to estimate the hyadraulic aperture of a DFN in such reservoirs (Figure 7B). Another key difference is that the above described techniques can be directly transferred into the DFN flow models that guide the production of fluids in hydrothermal reservoirs. Such models are highly reliable because they integrate all the structural geology, geophysical and hydraulic tests shown in

Figure 7A. Therefore, the need to fund research focused on data collection appears to be crucial to support geothermal production in naturally fractured sedimentary rocks that host hydrothermal reservoirs.

A different scenario and area for future research appear from the workflow shown in Figure 7B for HDR of igneous and metamorphic origin. Three steps of modelling are necessary after collection of fracture data in the field, borehole geophysical logging, and geomechanical data to determine the hydraulic parameters needed to move forward to production of geothermal fluids. Researchers need to build a DFN for flow determining the mechanical aperture through numerical modelling (Figure 7B; Bisdom et al., 2016; 2017). Additionally, either before fluid injection, or after by accounting for the enhanced fracturing pattern modelling is involved in the workflow. This review therefore shows that several datasets need to be collected to enable production of fluids in HDR systems. In these reservoirs (Figure 7B), collection of data need to be more heavily integrated with numerical modelling research that can be funded by governments and agencies.

6 Conclusion

Geothermal reservoirs modelling is challenging in a DFN framework due to the complexity of the structural geology, and the range of geomechanical and hydro-geophysical techniques required to represent fluid flow in heterogeneous geological media. This review for the first time summarizes different datasets while also discussing advantages/limitations and the potentialities of their combinations. The findings in this paper for DFN characterization will support models for the production of geothermal fluids, and can be summarized in the following five key points:

1. Structural scanlines and fracture statistics extracted from UAV surveys on outcropping analogues of reservoirs are the only approaches that provide the length of joints, bedding planes, and faults; these parameters guide and facilitate the stochastic generation of DFN models in lithified sedimentary, igneous, and metamorphic rocks.
2. The combination of ATV/FMI images and seismic attributes has also been proven to be an excellent approach that supports the stochastic generation of DFN models. The ATV/FMI images provide the only way to acquire orientation and the density of the fractures in the reservoirs, and the seismic attributes reveal the dominant trends of the joints and faults. Authors therefore envisage researchers to combine ATV logs images and seismic attributes with information from outcrop scanlines to acquire information on either the orientation or length of the fractures.
3. Computation of transmissivities from pumping tests and the number of hydraulically active fractures allows the hydraulic aperture to be determined; the aperture is a fundamental parameter that is needed to simulate flow in a network of discrete fractures. Pumping tests are used to compute the transmissvities in hydrothermal reservoirs, and the combinations of ATV logs and fluid temperature, and of electrical conductivities and velocity logs, determine the number of hydraulically active fractures.
4. Researchers need to determine geomechanical parameters (roughness, Young's modulus, Poisson's ratio, and

compressive strength) and estimate the apertures of rock discontinuities to inform DFN models in EGS/HDR. This information needs to be determined by laboratory testing on either intact or fractured samples of igneous and methamorphic rocks cored from the geothermal reservoir, and transferred to fractures that are correctly oriented with respect to the stress field.
5. Combinations of scanline surveys, fracture statistics from UAV, seismic attributes, geomechanical surveys, fluid logging and pumping tests still need to be evaluated by researchers before the parameters obtained from these techniques can be used for DFN flow modelling. This combination of technique has the potential to significantly improve fluid recovery in geothermal reservoirs.

Overall, networks of joints, bedding planes, and faults highly control fluid flow in deep saline aquifers and Hot Dry Rocks that host critical geothermal resources worldwide. Structural geologists, hydrogeologists, and reservoir engineers can find information in this review article on all the techniques used to characterize geothermal reservoirs as part of the preparation process for developing robust DFN flow models.

Author contributions

GM: Conceptualization, Writing–original draft. FL: Conceptualization, Writing–review and editing. JS: Conceptualization, Writing–review and editing.

Funding

Acknowledgments

Conflict of interest

The authors declare that the research was conducted in the absence of any commercial or financial relationships that could be construed as a potential conflict of interest.

Publisher's note

All claims expressed in this article are solely those of the authors and do not necessarily represent those of their affiliated organizations, or those of the publisher, the editors and the reviewers. Any product that may be evaluated in this article, or claim that may be made by its manufacturer, is not guaranteed or endorsed by the publisher.

References

Aabø, T. M., Dramsch, J. S., Würtzen, C. L., Seyum, S., and Welch, M. (2005). An integrated workflow for fracture characterization in chalk reservoirs, applied to the Kraka Field. *Mar. Pet. Geol.* 112, 104065. doi:10.1016/j.marpetgeo.2019.104065

Aabø, T. M., Oldfield, S., Yuan, H., Kammann, J., Sørensen, E. V., Stemmerik, L., et al. (2023). "Establishing a high resolution 3D fracture dataset in chalk: possibilities and obstacles working with outcrop data," in *Geomechanical controls on fracture development in Chalk and marl in the Danish North Sea*. Editors M. J. Welch and M. L. Luthje (Springer Nature).

Abe, A., and Horne, R. N. (2023). Investigating fracture network creation and stimulation mechanism of EGS reservoirs. *Geothermics* 107, 102606. doi:10.1016/j.geothermics.2022.102606

Abesser, C., Schincariol, R. A., Raymond, J., García-Gil, A., Drysdale, R., Piatek, A., et al. (2021). Case studies of geothermal system response to perturbations in groundwater flow and thermal regimes. *Groundwater* 61, 255–273. doi:10.1111/gwat.13086

Agemar, T., Weber, J., and Schulz, R. (2014). Deep geothermal energy production in Germany. *Energies* 7 (7), 4397–4416. doi:10.3390/en7074397

Agosta, F., Alessandroni, M., Antonellini, M., Tondi, E., and Giorgioni, M. (2010). From fractures to flow: a field-based quantitative analysis of an outcropping carbonate reservoir. *Tectonophysics* 490 (3-4), 197–213. doi:10.1016/j.tecto.2010.05.005

Akara, M. E. M., Reeves, D. M., and Parashar, R. (2020). Enhancing fracture-network characterization and discrete-fracture-network simulation with high-resolution surveys using unmanned aerial vehicles. *Hydrogeol. J.* 28 (7), 2285–2302. doi:10.1007/s10040-020-02178-y

Allmendinger, R. W., and Karabinos, P. (2023). Illuminating geology in areas of limited exposure using texture shading of lidar digital terrain models. *Geosphere* 19 (1), 163–178. doi:10.1130/ges02531.1

Andrews, B. J., Roberts, J. J., Shipton, Z. K., Bigi, S., Tartarello, M. C., and Johnson, G. (2019). How do we see fractures? Quantifying subjective bias in fracture data collection. *Solid earth.* 10 (2), 487–516. doi:10.5194/se-10-487-2019

Antonellini, M., Cilona, A., Tondi, E., Zambrano, M., and Agosta, F. (2014). Fluid flow numerical experiments of faulted porous carbonates, Northwest Sicily (Italy). *Mar. Pet. Geol.* 55, 186–201. doi:10.1016/j.marpetgeo.2013.12.003

Axelsson, G. (2010). Sustainable geothermal utilization–Case histories; definitions; research issues and modelling. *Geothermics* 39 (4), 283–291. doi:10.1016/j.geothermics.2010.08.001

Aydin, A. (2000). Fractures, faults, and hydrocarbon entrapment, migration and flow. *Mar. Pet. Geol.* 17 (7), 797–814. doi:10.1016/s0264-8172(00)00020-9

Bauer, J. F., Krumbholz, M., Meier, S., and Tanner, D. C. (2017). Predictability of properties of a fractured geothermal reservoir: the opportunities and limitations of an outcrop analogue study. *Geotherm. Energy* 5, 24–27. doi:10.1186/s40517-017-0081-0

Bauer, M., and Tóth, T. M. (2017). Characterization and DFN modelling of the fracture network in a Mesozoic karst reservoir: gomba oilfield, Paleogene Basin, Central Hungary. *J. Pet. Geol.* 40 (3), 319–334. doi:10.1111/jpg.12678

Bense, V. F., Gleeson, T., Loveless, S. E., Bour, O., and Scibek, J. (2013). Fault zone hydrogeology. *Earth Sci. Rev.* 127, 171–192. doi:10.1016/j.earscirev.2013.09.008

Bense, V. F., Shipton, Z. K., Kremer, Y., and Kampman, N. (2016). Fault zone hydrogeology: introduction to the special issue. *Geofluids* 16, 655–657. doi:10.1111/gfl.12205

Berkowitz, B. (2002). Characterizing flow and transport in fractured geological media: a review. *Adv. Water Resour.* 25 (8-12), 861–884. doi:10.1016/s0309-1708(02)00042-8

Bigi, S., Battaglia, M., Alemanni, A., Lombardi, S., Campana, A., Borisova, E., et al. (2013). CO2 flow through a fractured rock volume: insights from field data, 3D fractures representation and fluid flow modeling. *Int. J. Greenh. Gas. Control* 18, 183–199. doi:10.1016/j.ijggc.2013.07.011

Billi, A., Salvini, F., and Storti, F. (2003). The damage zone-fault core transition in carbonate rocks: implications for fault growth, structure and permeability. *J. Struct. Geol.* 25 (11), 1779–1794. doi:10.1016/s0191-8141(03)00037-3

Binda, G., Pozzi, A., Spanu, D., Livio, F., Trotta, S., and Bitonte, R. (2021). Integration of photogrammetry from unmanned aerial vehicles, field measurements and discrete fracture network modeling to understand groundwater flow in remote settings: test and comparison with geochemical markers in an Alpine catchment. *Hydrogeol. J.* 29 (3), 1203–1218. doi:10.1007/s10040-021-02304-4

Birsoy, Y. K., and Summers, W. K. (1980). Determination of aquifer parameters from step tests and intermittent pumping data. *Groundwater* 18 (2), 137–146. doi:10.1111/j.1745-6584.1980.tb03382.x

Bisdom, K., Bertotti, G., and Nick, H. M. (2016). The impact of in-situ stress and outcrop-based fracture geometry on hydraulic aperture and upscaled permeability in fractured reservoirs. *Tectonophysics* 690, 63–75. doi:10.1016/j.tecto.2016.04.006

Bisdom, K., Nick, H. M., and Bertotti, G. (2017). An integrated workflow for stress and flow modelling using outcrop-derived discrete fracture networks. *Comput. Geosci.* 103, 21–35. doi:10.1016/j.cageo.2017.02.019

Bixley, P. F., Clotworthy, A. W., and Mannington, W. I. (2009). Evolution of the Wairakei geothermal reservoir during 50 years of production. *Geothermics* 38 (1), 145–154. doi:10.1016/j.geothermics.2008.12.007

Blöcher, G., Reinsch, T., Henninges, J., Milsch, H., Regenspurg, S., Kummerow, J., et al. (2016). Hydraulic history and current state of the deep geothermal reservoir Groß Schönebeck. *Geothermics* 63, 27–43. doi:10.1016/j.geothermics.2015.07.008

Boersma, Q. D., Bruna, P. O., De Hoop, S., Vinci, F., Tehrani, A. M., and Bertotti, G. (2021). The impact of natural fractures on heat extraction from tight Triassic sandstones in the West Netherlands Basin: a case study combining well, seismic and numerical data. *Neth. J. Geosci.* 100, e6–e6. doi:10.1017/njg.2020.21

Bohnsack, D., Potten, M., Pfrang, D., Wolpert, P., and Zosseder, K. (2020). Porosity–permeability relationship derived from Upper Jurassic carbonate rock cores to assess the regional hydraulic matrix properties of the Malm reservoir in the South German Molasse Basin. *Geotherm. Energy.* 8 (1), 12–47. doi:10.1186/s40517-020-00166-9

Bossennec, C., Seib, L., Frey, M., Van Der Vaart, J., and Sass, I. (2022). Structural architecture and permeability patterns of crystalline reservoir rocks in the northern upper rhine graben: insights from surface analogues of the odenwald. *Energies* 15, 1310. doi:10.3390/en15041310

Bozzano, F., Martino, S., Montagna, A., and Prestininzi, A. (2012). Back analysis of a rock landslide to infer rheological parameters. *Eng. Geol.* 131, 45–56. doi:10.1016/j.enggeo.2012.02.003

Breede, K., Dzebisashvili, K., Liu, X., and Falcone, G. A. (2013). Systematic review of enhanced (or engineered) geothermal systems: past, present and future. *Geotherm. Energy.* 1, 1–27. doi:10.1186/2195-9706-1-4

Busby, J. (2014). Geothermal energy in sedimentary basins in the UK. *Hydrogeol. J.* 201422, 129–141. doi:10.1007/s10040-013-1054-4

Cant, J. L., Siratovich, P. A., Cole, J. W., Villeneuve, M. C., and Kennedy, B. M. (2018). Matrix permeability of reservoir rocks, Ngatamariki geothermal field, Taupo Volcanic Zone, New Zealand. *Geotherm. Energy.* 6 (1), 2–28. doi:10.1186/s40517-017-0088-6

Carminati, E., Aldega, L., Trippetta, F., Shaban, A., Narimani, H., and Sherkati, S. (2014). Control of folding and faulting on fracturing in the Zagros (Iran): the Kuh-e-Sarbalesh anticline. *J. Asian Earth Sci.* 79, 400–414. doi:10.1016/j.jseaes.2013.10.018

Caulk, R. A., and Tomac, I. (2017). Reuse of abandoned oil and gas wells for geothermal energy production. *Renew. Energ* 112, 388–397. doi:10.1016/j.renene.2017.05.042

Chiodini, G., Bini, G., Massaro, S., Caliro, S., Kanellopoulos, C., Tassi, F., et al. (2023). Ascent and decompressional boiling of geothermal liquids tracked by solute mass balances: a key to understand the hydrothermal explosions of Milos (Greece). *Front. Earth Sci.* 11, 1254547. doi:10.3389/feart.2023.1254547

Cho, Y. (2021). Stochastic discrete fracture network modeling in shale reservoirs via integration of seismic attributes and petrophysical data. *Interpretation* 9 (4), SG47–SG58. doi:10.1190/int-2020-0210.1

Cho, Y., Gibson, R. L., Jr, Lee, J., and Shin, C. (2019). Linear-slip discrete fracture network model and multiscale seismic wave simulation. *J. Appl. Geophys.* 164, 140–152. doi:10.1016/j.jappgeo.2019.03.006

Ciapała, B., Jurasz, J., Janowski, M., and Kępińska, B. (2021). Climate factors influencing effective use of geothermal resources in SE Poland: the Lublin trough. *Geotherm. Energy* 9, 1–16. doi:10.1186/s40517-021-00184-1

Clark, L. (1977). The analysis and planning of step drawdown tests. *Quart. J. Eng. Geol. Hydrogeol.* 10 (2), 125–143. doi:10.1144/gsl.qjeg.1977.010.02.03

Clauser, C. (1992). Permeability of crystalline rocks. *Eos Trans. Am. Geophys. Union.* 73 (21), 233–238. doi:10.1029/91eo00190

Colombera, L., Mountney, N. P., Medici, G., and West, L. J. (2019). The geometry of fluvial channel bodies: empirical characterization and implications for object-based

models of the subsurface. *Am. Assoc. Pet. Geol. Bull.* 103 (4), 905–929. doi:10.1306/10031817417

De Franco, R., Petracchini, L., Scrocca, D., Caielli, G., Montegrossi, G., Santilano, A., et al. (2019). Synthetic seismic reflection modelling in a supercritical geothermal system: an image of the k-horizon in the Larderello field (Italy). *Geofluids* 21. doi:10.1155/2019/8492453

Dijk, P., Berkowitz, B., and Bendel, P. (1999). Investigation of flow in water-saturated rock fractures using nuclear magnetic resonance imaging (NMRI). *Water Resour. Res.* 35 (2), 347–360. doi:10.1029/1998wr900044

Doran, H. R., Renaud, T., Falcone, G., Pan, L., and Verdin, P. G. (2021). Modelling an unconventional closed-loop deep borehole heat exchanger (DBHE): sensitivity analysis on the Newberry volcanic setting. *Geotherm. Energy* 9 (1), 4–24. doi:10.1186/s40517-021-00185-0

Dorhjie, D. B., Yusupov, R., Krutko, V., and Cheremisin, A. (2022). Deviation from Darcy law in porous media due to reverse osmosis: pore-scale approach. *Energies* 15 (18), 6656. doi:10.3390/en15186656

Dragoni, M., and Santini, S. (2022). Contribution of the 2010 maule megathrust earthquake to the heat flow at the Peru-Chile trench. *Energies* 15, 2253. doi:10.3390/en15062253

Eden, R. N., and Hazel, C. P. (1973). *Civil engineering transactions*. Sydney, Australia: Institution of Engineers.Computer and graphical analysis of variable discharge pumping tests of wells

Eldosouky, A. M., Ekwok, S. E., Ben, U. C., Ulem, C. A., Abdelrahman, K., Gomez-Ortiz, D., et al. (2023). Appraisal of geothermal potentials of some parts of the Abakaliki Anticlinorium and adjoining areas (Southeast Nigeria) using magnetic data. *Front. Earth Sci.* 11, 1216198. doi:10.3389/feart.2023.1216198

Fadel, M., Reinecker, J., Bruss, D., and Moeck, I. (2022). Causes of a premature thermal breakthrough of a hydrothermal project in Germany. *Geothermics* 105, 102523. doi:10.1016/j.geothermics.2022.102523

Fazio, M., Ibemesi, P., Benson, P., Bedoya-González, D., and Sauter, M. (2021). The role of rock matrix permeability in controlling hydraulic fracturing in sandstones. *Rock Mech. Rock Eng.* 54 (10), 5269–5294. doi:10.1007/s00603-021-02580-2

Filipovich, R., Báez, W., Groppelli, G., Ahumada, F., Aldega, L., Becchio, R., et al. (2020). Geological map of the Tocomar basin (Puna Plateau, NW Argentina). Implication for the geothermal system investigation. *Energies* 13 (20), 5492. doi:10.3390/en13205492

Fiorucci, M., Martino, S., Bozzano, F., and Prestininzi, A. (2020). Comparison of approaches for data analysis of multi-parametric monitoring systems: insights from the Acuto test-site (Central Italy). *Appl. Sci.* 10 (21), 7658. doi:10.3390/app10217658

Förster, A., Förster, H. J., and Krentz, O. (2018). Exploration of the enhanced geothermal system (EGS) potential of crystalline rocks for district heating (Elbe Zone, Saxony, Germany). *Int. J. Earth Sci.* 107, 89–101. doi:10.1007/s00531-016-1429-6

Fox, D. B., Koch, D. L., and Tester, J. W. (2015). The effect of spatial aperture variations on the thermal performance of discretely fractured geothermal reservoirs. *Geotherm. Energy* 3, 21–29. doi:10.1186/s40517-015-0039-z

Francioni, M., Antonaci, F., Sciarra, N., Robiati, C., Coggan, J., Stead, D., et al. (2020). Application of unmanned aerial vehicle data and discrete fracture network models for improved rockfall simulations. *Remote Sensing* 12 (12), 2053.

Freitag, S., Klaver, J., Malai, I. S., Klitzsch, N., Urai, J. L., Stollhofen, H., et al. (2022). Petrophysical characterization, BIB-SEM imaging, and permeability models of tight carbonates from the Upper Jurassic (Malm ß), SE Germany. *Geotherm. Energy* 10 (1), 30–40. doi:10.1186/s40517-022-00239-x

Frosch, G. P., Tillich, J. E., Haselmeier, R., Holz, M., and Althaus, E. (2000). Probing the pore space of geothermal reservoir sandstones by nuclear magnetic resonance. *Geothermics* 29 (6), 671–687. doi:10.1016/s0375-6505(00)00031-6

Gaillot, P., Brewer, T., Pezard, P., and Yeh, E. C. (2007). Borehole imaging tools—principles and applications. *Sci. Drill.* 5, 1–4.

García-Gil, A., Mejías Moreno, M., Garrido Schneider, E., Marazuela, M. Á., Abesser, C., Mateo Lázaro, J., et al. (2020). Nested shallow geothermal systems. *Sustainability* 12 (12), 5152. doi:10.3390/su12125152

Genter, A., Castaing, C., Dezayes, C., Tenzer, H., Traineau, H., and Villemin, T. (1997). Comparative analysis of direct (core) and indirect (borehole imaging tools) collection of fracture data in the Hot Dry Rock Soultz reservoir (France). *J. Geophys. Res. Solid Earth* 102 (B7), 15419–15431. doi:10.1029/97jb00626

Giordan, D., Adams, M. S., Aicardi, I., Alicandro, M., Allasia, P., Baldo, M., et al. (2020). The use of unmanned aerial vehicles (UAVs) for engineering geology applications. *Bull. Eng. Geol. Environ.* 79, 3437–3481. doi:10.1007/s10064-020-01766-2

Giuffrida, A., Agosta, F., Rustichelli, A., Panza, E., La Bruna, V., Eriksson, M., et al. (2020). Fracture stratigraphy and DFN modelling of tight carbonates, the case study of the Lower Cretaceous carbonates exposed at the Monte Alpi (Basilicata, Italy). *Mar. Pet. Geol.* 112, 104045. doi:10.1016/j.marpetgeo.2019.104045

Goupil, M., Heap, M. J., and Baud, P. (2022). Permeability anisotropy in sandstones from the Soultz-sous-Forêts geothermal reservoir (France): implications for large-scale fluid flow modelling. *Geotherm. Energy* 10, 32. doi:10.1186/s40517-022-00243-1

Gudmundsson, A. (2022). Transport of geothermal fluids along dikes and fault zones. *Energies* 15, 7106. doi:10.3390/en15197106

Guerriero, V., Vitale, S., Ciarcia, S., and Mazzoli, S. (2011). Improved statistical multi-scale analysis of fractured reservoir analogues. *Tectonophysics* 504 (1-4), 14–24. doi:10.1016/j.tecto.2011.01.003

Guo, J., Zheng, J., Lü, Q., Xiao, Z., and Liu, T. (2022). An analysis of trace information of different-shaped fracture networks having a same fracture intensity (P 32). *KSCE J. Civ. Eng.* 26 (10), 4265–4275. doi:10.1007/s12205-022-1165-3

Haffen, S., Géraud, Y., Diraison, M., and Dezayes, C. (2013). Determination of fluid-flow zones in a geothermal sandstone reservoir using thermal conductivity and temperature logs. *Geothermics* 46, 32–41. doi:10.1016/j.geothermics.2012.11.001

Hale, S., Ries, X., Jaeggi, D., and Blum, P. (2021). Mechanical and hydraulic properties of the excavation damaged zone (EDZ) in the Opalinus Clay of the Mont Terri rock laboratory, Switzerland. *Solid earth.* 12 (7), 1581–1600. doi:10.5194/se-12-1581-2021

Hantush, M. S. (1966). Analysis of data from pumping tests in anisotropic aquifers. *J. Geophys. Res.* 71 (2), 421–426. doi:10.1029/jz071i002p00421

Hartmann, A., Goldscheider, N., Wagener, T., Lange, J., and Weiler, M. (2014). Karst water resources in a changing world: review of hydrological modeling approaches. *Rev. Geophys.* 52 (3), 218–242. doi:10.1002/2013rg000443

Hayashi, K., Willis-Richards, J., Hopkirk, R. J., and Niibori, Y. (1999). Numerical models of HDR geothermal reservoirs—a review of current thinking and progress. *Geothermics* 28, 507–518. doi:10.1016/s0375-6505(99)00026-7

Hering, P., Lindenfeld, M., and Rümpker, G. (2023). Automatized localization of induced geothermal seismicity using robust time-domain array processing. *Front. Earth Sci.* 11, 1217587. doi:10.3389/feart.2023.1217587

Hicks, W. G., and Berry, J. E. (1956). Application of continuous velocity logs to determination of fluid saturation of reservoir rocks. *Geophysics* 21 (3), 739–754. doi:10.1190/1.1438267

Hitchmough, A. M., Riley, M. S., Herbert, A. W., and Tellam, J. H. (2007). Estimating the hydraulic properties of the fracture network in a sandstone aquifer. *J. Contam. Hydrol.* 93 (1-4), 38–57. doi:10.1016/j.jconhyd.2007.01.012

Huang, Y., Cheng, Y., Ren, L., Tian, F., Pan, S., Wang, K., et al. (2022). Assessing the geothermal resource potential of an active oil field by integrating a 3D geological model with the hydro-thermal coupled simulation. *Front. Earth Sci.* 9, 787057. doi:10.3389/feart.2021.787057

Hyman, J. D., Karra, S., Makedonska, N., Gable, C. W., Painter, S. L., and Viswanathan, H. S. (2015). dfnWorks: a discrete fracture network framework for modeling subsurface flow and transport. *Comput. Geosci* 84, 10–19. doi:10.1016/j.cageo.2015.08.001

Jain, C., Vogt, C., and Clauser, C. (2015). Maximum potential for geothermal power in Germany based on engineered geothermal systems. *Geotherm. Energy* 3 (1), 15–20. doi:10.1186/s40517-015-0033-5

Janiga, D., Kwaśnik, J., and Wojnarowski, P. (2022). Utilization of discrete fracture network (DFN) in modelling and simulation of a horizontal well-doublet enhanced geothermal system (EGS) with sensitivity analysis of key production parameters. *Energies* 15 (23), 9020. doi:10.3390/en15239020

Ji, S. H., and Koh, Y. K. (2017). Appropriate domain size for groundwater flow modeling with a discrete fracture network model. *Groundwater* 55 (1), 51–62. doi:10.1111/gwat.12435

Kana, A. A., West, L. J., and Clark, R. A. (2013). Fracture aperture and fill characterization in a limestone quarry using GPR thin-layer AVA analysis. *Near Surf. Geophys.* 11 (3), 293–306. doi:10.3997/1873-0604.2012066

Kawecki, M. (1995). Meaningful interpretation of step-drawdown tests. *Groundwater* 33 (1), 23–32. doi:10.1111/j.1745-6584.1995.tb00259.x

Kittilä, A., Jalali, M., Saar, M. O., and Kong, X. Z. (2020a). Solute tracer test quantification of the effects of hot water injection into hydraulically stimulated crystalline rock. *Geotherm. Energy* 8 (1), 17–27. doi:10.1186/s40517-020-00172-x

Kittilä, A., Mohammadreza, R. J., Somogyvári, M., Evans, K. F., Saar, M. O., and Kong, X. Z. (2020b). Characterization of the effects of hydraulic stimulation with tracer-based temporal moment analysis and tomographic inversion. *Geothermics* 86, 101820. doi:10.1016/j.geothermics.2020.101820

Klinka, T., and Gutierrez, A. (2020). *OUAIP Manual – tool to assist in pumping tests Interpretation*. Orléans, France. BRGM/RP-69388-FR.

Kong, Y., Pang, Z., Shao, H., Hu, S., and Kolditz, O. (2014). Recent studies on hydrothermal systems in China: a review. *Geotherm. Energy* 2, 19–12. doi:10.1186/s40517-014-0019-8

Kristensen, L., Hjuler, M. L., Frykman, P., Olivarius, M., Weibel, R., Nielsen, L. H., et al. (2016). Pre-drilling assessments of average porosity and permeability in the geothermal reservoirs of the Danish area. *Geotherm. Energy* 4 (1), 6–27. doi:10.1186/s40517-016-0048-6

Lancia, M., Saroli, M., and Petitta, M. (2018). A double scale methodology to investigate flow in karst fractured media via numerical analysis: the Cassino plain case study (central Apennine, Italy). *Geofluids* 1, 1–12. doi:10.1155/2018/2937105

Lancia, M., Su, H., Tian, Y., Xu, J., Andrews, C., Lerner, D. N., et al. (2020). Hydrogeology of the pearl river delta, southern China. *J. Maps* 16 (2), 388–395. doi:10.1080/17445647.2020.1761903

Lato, M. J., Diederichs, M. S., and Hutchinson, D. J. (2010). Bias correction for view-limited Lidar scanning of rock outcrops for structural characterization. *Rock Mech. Rock Eng.* 43, 615–628. doi:10.1007/s00603-010-0086-5

Lee, H. S., and Ahn, K. W. (2004). A prototype of digital photogrammetric algorithm for estimating roughness of rock surface. *Geosci. J.* 8, 333–341. doi:10.1007/bf02910253

Lemieux, J. M., Kirkwood, D., and Therrien, R. (2009). Fracture network analysis of the St-Eustache quarry, Quebec, Canada, for groundwater resources management. *Can. Geotech. J.* 46 (7), 828–841. doi:10.1139/t09-022

Lennox, D. H. (1966). Analysis and application of step-drawdown test. *J. Hydraul. Div.* 92 (6), 25–48. doi:10.1061/jyceaj.0001558

Lepillier, B., Bruna, P. O., Bruhn, D., Bastesen, E., Daniilidis, A., Garcia, Ó., et al. (2020). From outcrop scanlines to discrete fracture networks, an integrative workflow. *J. Struct. Geol.* 133, 103992. doi:10.1016/j.jsg.2020.103992

Lepillier, B., Daniilidis, A., Doonechaly Gholizadeh, N., Bruna, P. O., Kummerow, J., and Bruhn, D. (2019). A fracture flow permeability and stress dependency simulation applied to multi-reservoirs, multi-production scenarios analysis. *Geotherm. Energy* 7 (1), 24–16. doi:10.1186/s40517-019-0141-8

Li, H. B., Zhao, J., and Li, T. J. (1999). Triaxial compression tests on a granite at different strain rates and confining pressures. *Int. J. Rock Mech. Min. Sci.* 36 (8), 1057–1063. doi:10.1016/s1365-1609(99)00120-3

Lima, M. G., Vogler, D., Querci, L., Madonna, C., Hattendorf, B., Saar, M. O., et al. (2019). Thermally driven fracture aperture variation in naturally fractured granites. *Geotherm. Energy* 7 (1), 23–28. doi:10.1186/s40517-019-0140-9

Liotta, D., Brogi, A., Ruggieri, G., and Zucchi, M. (2021). Fossil vs. Active geothermal systems: a field and laboratory method to disclose the relationships between geothermal fluid flow and geological structures at depth. *Energies* 14, 933. doi:10.3390/en14040933

Lu, J., Li, C., Wang, M., and Zhang, C. (2023). Review of deep fluids in sedimentary basins and their influence on resources, with a focus on oil and geothermal exploitation. *Front. Earth Sci.* 10, 896629. doi:10.3389/feart.2022.896629

Ma, Y., Gan, Q., Zhang, Y., and Zhou, L. (2022). Numerical simulation of the heat production potential of Guide Basin in China considering the heterogeneity and anisotropy of the reservoir. *Geothermics* 105, 102508. doi:10.1016/j.geothermics.2022.102508

Majorowicz, J. (2021). Review of the heat flow mapping in polish sedimentary basin across different tectonic terrains. *Energies* 14, 6103. doi:10.3390/en14196103

Majorowicz, J., and Grasby, S. E. (2021). Deep geothermal heating potential for the communities of the western Canadian sedimentary basin. *Energies* 14, 706. doi:10.3390/en14030706

Maldaner, C. H., Quinn, P. M., Cherry, J. A., and Parker, B. L. (2018). Improving estimates of groundwater velocity in a fractured rock borehole using hydraulic and tracer dilution methods. *J. Contam. Hydrol.* 214, 75–86. doi:10.1016/j.jconhyd.2018.05.003

Manzella, A., Bonciani, R., Allansdottir, A., Botteghi, S., Donato, A., Giamberini, S., et al. (2018). Environmental and social aspects of geothermal energy in Italy. *Geothermics* 72, 232–248. doi:10.1016/j.geothermics.2017.11.015

Marchesini, B., Garofalo, P. S., Menegon, L., Mattila, J., and Viola, G. (2019). Fluid-mediated, brittle–ductile deformation at seismogenic depth–Part 1: fluid record and deformation history of fault veins in a nuclear waste repository (Olkiluoto Island, Finland). *Solid earth.* 10 (3), 809–838. doi:10.5194/se-10-809-2019

Marmoni, G. M., Fiorucci, M., Grechi, G., and Martino, S. (2020). Modelling of thermo-mechanical effects in a rock quarry wall induced by near-surface temperature fluctuations. *Int. J. Rock Mech. Min. Sci.* 134, 104440. doi:10.1016/j.ijrmms.2020.104440

Massiot, C., McNamara, D. D., and Lewis, B. (2015). Processing and analysis of high temperature geothermal acoustic borehole image logs in the Taupo Volcanic Zone, New Zealand. *Geothermics* 53, 190–201. doi:10.1016/j.geothermics.2014.05.010

Mathias, S. A., and Todman, L. C. (2010). Step-drawdown tests and the Forchheimer equation. *Water Resour. Res.* 46 (7). doi:10.1029/2009wr008635

Mazzoli, S. (2022). Geothermal energy and structural geology. *Energies* 15 (21), 8074. doi:10.3390/en15218074

Medici, G., Smeraglia, L., Torabi, A., and Botter, C. (2021). Review of modeling approaches to groundwater flow in deformed carbonate aquifers. *Groundwater* 59 (3), 334–351. doi:10.1111/gwat.13069

Medici, G., and West, L. J. (2023). Reply to discussion on 'Review of groundwater flow and contaminant transport modelling approaches for the Sherwood Sandstone aquifer, UK; insights from analogous successions worldwide' by Medici and West (QJEGH, 55, qjegh2021-176). *Q. J. Eng. Geol. Hydrogeol.* 56 (1), qjegh2022–097. doi:10.1144/qjegh2022-097

Medici, G., West, L. J., and Banwart, S. A. (2019b). Groundwater flow velocities in a fractured carbonate aquifer-type: implications for contaminant transport. *J. Contam. Hydrol.* 222, 1–16. doi:10.1016/j.jconhyd.2019.02.001

Medici, G., West, L. J., and Mountney, N. P. (2016). Characterizing flow pathways in a sandstone aquifer: tectonic vs sedimentary heterogeneities. *J. Contam. Hydrol.* 194, 36–58. doi:10.1016/j.jconhyd.2016.09.008

Medici, G., West, L. J., and Mountney, N. P. (2018). Characterization of a fluvial aquifer at a range of depths and scales: the triassic st bees sandstone formation, cumbria, UK. *Hydrogeol. J.* 26 (2), 565–591. doi:10.1007/s10040-017-1676-z

Medici, G., West, L. J., Mountney, N. P., and Welch, M. (2019a). Permeability of rock discontinuities and faults in the Triassic Sherwood Sandstone Group (UK): insights for management of fluvio-aeolian aquifers worldwide. *Hydrogeol. J.* 27 (8), 2835–2855. doi:10.1007/s10040-019-02035-7

Melouah, O., Ebong, E. D., Abdelrahman, K., and Eldosouky, A. M. (2023). Lithospheric structural dynamics and geothermal modeling of the Western Arabian Shield. *Sci. Rep.* 13 (1), 11764. doi:10.1038/s41598-023-38321-4

Melouah, O., Eldosouky, A. M., and Ebong, E. D. (2021b). Crustal architecture, heat transfer modes and geothermal energy potentials of the Algerian Triassic provinces. *Geothermics* 96, 102211. doi:10.1016/j.geothermics.2021.102211

Melouah, O., Steinmetz, R. L. L., and Ebong, E. D. (2021a). Deep crustal architecture of the eastern limit of the west african craton: ougarta range and western Algerian sahara. *J. Afr. Earth Sci.* 183, 104321. doi:10.1016/j.jafrearsci.2021.104321

Minissale, A. (1991). The Larderello geothermal field: a review. *Earth-Sci. Rev.* 31 (2), 133–151. doi:10.1016/0012-8252(91)90018-b

Młynarczuk, M. (2010). Description and classification of rock surfaces by means of laser profilometry and mathematical morphology. *Int. J. Rock Mech. Min. Sci.* 47 (1), 138–149. doi:10.1016/j.ijrmms.2009.09.004

Mogi, K. (1971). Fracture and flow of rocks under high triaxial compression. *J. Geophys. Res.* 76 (5), 1255–1269. doi:10.1029/jb076i005p01255

Müller, C., Siegesmund, S., and Blum, P. (2010). Evaluation of the representative elementary volume (REV) of a fractured geothermal sandstone reservoir. *Environ. Earth Sci.* 61, 1713–1724. doi:10.1007/s12665-010-0485-7

Munn, J. D., Maldaner, C. H., Coleman, T. I., and Parker, B. L. (2020). Measuring fracture flow changes in a bedrock aquifer due to open hole and pumped conditions using active distributed temperature sensing. *Water Resour. Res.* 56 (10). doi:10.1029/2020wr027229

Okoroafor, E. R., Smith, C. M., Ochie, K. I., Nwosu, C. J., Gudmundsdottir, H., and Aljubran, M. J. (2022). Machine learning in subsurface geothermal energy: two decades in review. *Geothermics* 102, 102401. doi:10.1016/j.geothermics.2022.102401

Oron, A. P., and Berkowitz, B. (1998). Flow in rock fractures: the local cubic law assumption reexamined. *Water Resour. Res.* 34 (11), 2811–2825. doi:10.1029/98wr02285

Paillet, F. L., and Pedler, W. H. (1996). Integrated borehole logging methods for wellhead protection applications. *Eng. Geol.* 42 (2-3), 155–165. doi:10.1016/0013-7952(95)00077-1

Paillet, F. L., Williams, J. H., Oki, D. S., and Knutson, K. D. (2002). Comparison of formation and fluid-column logs in a heterogeneous basalt aquifer. *Groundwater* 40 (6), 577–585. doi:10.1111/j.1745-6584.2002.tb02544.x

Pehme, P. E., Greenhouse, J. P., and Parker, B. L. (2007). The active line source temperature logging technique and its application in fractured rock hydrogeology. *J. Environ. Eng. Geophys.* 12 (4), 307–322. doi:10.2113/jeeg12.4.307

Pehme, P. E., Parker, B. L., Cherry, J. A., Molson, J. W., and Greenhouse, J. P. (2013). Enhanced detection of hydraulically active fractures by temperature profiling in lined heated bedrock boreholes. *J. Hydrol.* 484, 1–15. doi:10.1016/j.jhydrol.2012.12.048

Przybycin, A. M., Scheck-Wenderoth, M., and Schneider, M. (2017). The origin of deep geothermal anomalies in the German Molasse Basin: results from 3D numerical models of coupled fluid flow and heat transport. *Geotherm. Energy* 5, 1–28. doi:10.1186/s40517-016-0059-3

Quinn, P., Cherry, J. A., and Parker, B. L. (2015). Combined use of straddle packer testing and FLUTe profiling for hydraulic testing in fractured rock boreholes. *J. Hydrol.* 524, 439–454. doi:10.1016/j.jhydrol.2015.03.008

Quinn, P. M., Cherry, J. A., and Parker, B. L. (2020). Relationship between the critical Reynolds number and aperture for flow through single fractures: evidence from published laboratory studies. *J. Hydrol.* 581, 124384. doi:10.1016/j.jhydrol.2019.124384

Raef, A., Gad, S., and Tucker-Kulesza, S. (2015). Multichannel analysis of surface-waves and integration of downhole acoustic televiewer imaging, ultrasonic vs and Vp, and vertical seismic profiling in an NEHRP-standard classification, South of Concordia, Kansas, USA. *J. Appl. Geophys.* 121, 149–161. doi:10.1016/j.jappgeo.2015.08.005

Randolph, J. B., and Saar, M. O. (2011). Coupling carbon dioxide sequestration with geothermal energy capture in naturally permeable, porous geologic formations: implications for CO2 sequestration. *Energy Procedia* 4, 2206–2213. doi:10.1016/j.egypro.2011.02.108

Renshaw, C. E. (1995). On the relationship between mechanical and hydraulic apertures in rough-walled fractures. *J. Geophys. Res. Solid Earth.* 100, 24629–24636. doi:10.1029/95jb02159

Romano, V., Bigi, S., Carnevale, F., Hyman, J. D. H., Karra, S., Valocchi, A. J., et al. (2020). Hydraulic characterization of a fault zone from fracture distribution. *J. Struct. Geol.* 135, 104036. doi:10.1016/j.jsg.2020.104036

Romm, E. S. (1966). *Flow characteristics in fractured rocks*. Moscow, Russia: Nedra.

Rosberg, J. E., and Erlström, M. (2021). Evaluation of deep geothermal exploration drillings in the crystalline basement of the Fennoscandian Shield Border Zone in south Sweden. Geotherm. *Energy* 9 (1), 1–25. doi:10.1186/s40517-021-00203-1

Roshan, H., Li, D., Canbulat, I., and Regenauer-Lieb, K. (2023). Borehole deformation based *in situ* stress estimation using televiewer data. *J. Rock Mechan. Geotech. Eng.*, 15, 2475–2481. doi:10.1016/j.jrmge.2022.12.016

Rubio-Maya, C., Díaz, V. A., Martínez, E. P., and Belman-Flores, J. M. (2015). Cascade utilization of low and medium enthalpy geothermal resources– A review. *Renew. Sustain. Energy Rev.* 52, 689–716. doi:10.1016/j.rser.2015.07.162

Rybach, L. (2022). Geothermal heat pump production sustainability—the basis of the Swiss GHP success story. *Energies* 15 (21), 7870. doi:10.3390/en15217870

Salazar, S. S., Muñoz, Y., and Ospino, A. (2017). Analysis of geothermal energy as an alternative source for electricity in Colombia. *Geotherm. Energy* 5 (1), 27–12. doi:10.1186/s40517-017-0084-x

Saleem, Z. (1970). A computer method for pumping-test analysis. *Groundwater* 8 (5), 21–24. doi:10.1111/j.1745-6584.1970.tb01318.x

Salvini, R., Mastrorocco, G., Seddaiu, M., Rossi, D., and Vanneschi, C. (2017). The use of an unmanned aerial vehicle for fracture mapping within a marble quarry (Carrara, Italy): photogrammetry and discrete fracture network modelling. *Geomat. Nat. Hazards Risk.* 8 (1), 34–52. doi:10.1080/19475705.2016.1199053

Santini, S., Basilici, M., Invernizzi, C., Jablonska, D., Mazzoli, S., Megna, A., et al. (2021). Controls of radiogenic heat and moho geometry on the thermal setting of the marche region (Central Italy): an analytical 3D geothermal model. *Energies* 14, 6511. doi:10.3390/en14206511

Santini, S., Basilici, M., Invernizzi, C., Mazzoli, S., Megna, A., Pierantoni, P. P., et al. (2020). Thermal structure of the northern outer albanides and adjacent adriatic crustal sector, and implications for geothermal energy systems. *Energies* 13, 6028. doi:10.3390/en13226028

Sari, M., and Karpuz, C. (2006). Rock variability and establishing confining pressure levels for triaxial tests on rocks. *Int. J. Rock Mech. Min. Sci.* 43 (2), 328–335. doi:10.1016/j.ijrmms.2005.06.010

Schilirò, L., Robiati, C., Smeraglia, L., Vinci, F., Iannace, A., Parente, M., et al. (2022). An integrated approach for the reconstruction of rockfall scenarios from UAV and satellite-based data in the Sorrento Peninsula (southern Italy). *Eng. Geol.* 308, 106795. doi:10.1016/j.enggeo.2022.106795

Schneider, S., Eichkitz, C. G., Schreilechner, M. G., and Davis, J. C. (2016). Interpretation of fractured zones using seismic attributes — case study from Teapot Dome, Wyoming, USA. *Wyo. USA. Interpret.* 4 (2), T249–T260. doi:10.1190/int-2015-0210.1

Selroos, J. O., Walker, D. D., Ström, A., Gylling, B., and Follin, S. (2002). Comparison of alternative modelling approaches for groundwater flow in fractured rock. *J. Hydrol.* 257 (1-4), 174–188. doi:10.1016/s0022-1694(01)00551-0

Senel, O., Will, R., and Butsch, R. J. (2014). Integrated reservoir modeling at the Illinois Basin–Decatur project. *Greenh. Gases Sci. Technol.* 4 (5), 662–684. doi:10.1002/ghg.1451

Shafiq, M. U., and Mahmud, H. B. (2017). Sandstone matrix acidizing knowledge and future development. *J. Pet. Explor. Prod. Technol.* 7 (4), 1205–1216. doi:10.1007/s13202-017-0314-6

Shang, J. (2020). Rupture of veined granite in polyaxial compression: insights from three-dimensional discrete element method modeling. *J. Geophys. Res. Solid Earth.* 125 (2), e2019JB019052. doi:10.1029/2019jb019052

Shang, J., Hencher, S. R., and West, L. J. (2016). Tensile strength of geological discontinuities including incipient bedding, rock joints and mineral veins. *Rock Mechan. Rock Eng.* 49, 4213–4225. doi:10.1007/s00603-016-1041-x

Shang, J., West, L. J., Hencher, S. R., and Zhao, Z. (2018). Geological discontinuity persistence: implications and quantification. *Eng. Geol.* 241, 41–54. doi:10.1016/j.enggeo.2018.05.010

Smeraglia, L., Mercuri, M., Tavani, S., Pignalosa, A., Kettermann, M., Billi, A., et al. (2021). 3D Discrete Fracture Network (DFN) models of damage zone fluid corridors within a reservoir-scale normal fault in carbonates: multiscale approach using field data and UAV imagery. *Mar. Pet. Geol.* 26, 104902. doi:10.1016/j.marpetgeo.2021.104902

Smit, F. W. H., and Welch, M. J. (2023). "Improved visualization of structural deformation on the Kraka structure (Danish Central Graben) with color-processed seismic data," in *Geomechanical controls on fracture development in Chalk and marl in the Danish North Sea*. Editors M. J. Welch and M. L. Luthje (Springer Nature).

Stork, A., Lund, B., David, A., Clarke, A., Nygren, C., Johansson, S., et al. (2020). *Comparison of the capabilities of DAS fibre-optic technologies and geophones for VSP surveys*, 1. Utrecht, Netherlands: EAGE Publ., 1–5.

Streetly, M., Chakrabarty, C., and McLeod, R. (2000). Interpretation of pumping tests in the sherwood sandstone group, sellafield, cumbria, UK. *Q. J. Eng. Geol. Hydrogeol.* 33 (4), 281–299. doi:10.1144/qjegh.33.4.281

Streetly, M. J., and Heathcote, J. (2018). Advances in groundwater system measurement and monitoring documented in 50 years of QJEGH. *Q. J. Eng. Geol. Hydrogeol.* 51 (2), 139–155. doi:10.1144/qjegh2016-140

Streetly, M. J., Heathcote, J. A., and Degnan, P. (2006). Estimation of vertical diffusivity from seasonal fluctuations in groundwater pressures in deep boreholes near Sellafield, NW England. *Geol. Soc. Lond. Spec. Publ.* 263 (1), 155–167. doi:10.1144/gsl.sp.2006.263.01.08

Szanyi, J., and Kovács, B. (2010). Utilization of geothermal systems in South-East Hungary. *Geothermics* 39 (4), 357–364. doi:10.1016/j.geothermics.2010.09.004

Tavani, S., Billi, A., Corradetti, A., Mercuri, M., Bosman, A., Cuffaro, M., et al. (2022). Smartphone assisted fieldwork: towards the digital transition of geoscience fieldwork using LiDAR-equipped iPhones. *Earth-Sci. Rev.* 227, 103969. doi:10.1016/j.earscirev.2022.103969

Tellam, J. H., and Barker, R. D. (2006). Towards prediction of saturated-zone pollutant movement in groundwaters in fractured permeable-matrix aquifers: the case of the UK Permo-Triassic sandstones. *Geol. Soc. Lond. Spec. Publ.* 263 (1), 1–48. doi:10.1144/gsl.sp.2006.263.01.01

Terzaghi, R. D. (1965). Sources of error in joint surveys. *Geotechnique* 15 (3), 287–304. doi:10.1680/geot.1965.15.3.287

Torabi, A., Alaei, B., and Ellingsen, T. S. S. (2018). Faults and fractures in basement rocks, their architecture, petrophysical and mechanical properties. *J. Struct. Geol.* 117, 256–263. doi:10.1016/j.jsg.2018.07.001

Tsang, Y. W. (1984). The effect of tortuosity on fluid flow through a single fracture. *Water Resour. Res.* 20 (9), 1209–1215. doi:10.1029/wr020i009p01209

Tuckey, Z. (2022). An integrated UAV photogrammetry-discrete element investigation of jointed Triassic sandstone near Sydney, Australia. *Eng. Geol.* 297, 106517. doi:10.1016/j.enggeo.2022.106517

Turner, J. P., Healy, D., Hillis, R. R., and Welch, M. J. (2017). Geomechanics and geology: introduction. *Geol. Soc. Lond. Spec. Publ.* 458 (1), 1–5. doi:10.1144/sp458.15

Villeneuve, M. C., Heap, M. J., Kushnir, A. R., Qin, T., Baud, P., Zhou, G., et al. (2018). Estimating *in situ* rock mass strength and elastic modulus of granite from the Soultz-sous-Forêts geothermal reservoir (France). *Geotherm. Energy* 6, 11–29. doi:10.1186/s40517-018-0096-1

Vitale, S., Dati, F., Mazzoli, S., Ciarcia, S., Guerriero, V., and Iannace, A. (2012). Modes and timing of fracture network development in poly-deformed carbonate reservoir analogues, Mt. Chianello, southern Italy. *J. Struct. Geol.* 37, 223–235. doi:10.1016/j.jsg.2012.01.005

Wealthall, G. P., Steele, A., Bloomfield, J. P., Moss, R. H., and Lerner, D. N. (2001). Sediment filled fractures in the Permo-Triassic sandstones of the Cheshire Basin: observations and implications for pollutant transport. *J. Contam. Hydrol.* 50 (1-2), 41–51. doi:10.1016/s0169-7722(01)00104-8

Welch, M. J. (2023). "Using geomechanical models to simulate the growth of the fracture network in the Ekofisk Formation of the Kraka structure, Danish Central Graben," in *Geomechanical controls on fracture development in Chalk and marl in the Danish North Sea*. Editors M. J. Welch and M. L. Luthje (Springer Nature).

Welch, M. J., Lüthje, M., and Oldfield, S. J. (2022). DFN Generator v2. 0: a new tool to model the growth of large-scale natural fracture networks using fundamental geomechanics. *Geosci. Model. Dev. Discuss.* doi:10.5194/gmd-2022-22

Wight, N. M., and Bennett, N. S. (2015). Geothermal energy from abandoned oil and gas wells using water in combination with a closed wellbore. *Appl. Therm. Eng.* 89, 908–915. doi:10.1016/j.applthermaleng.2015.06.030

Williams, J. H., and Johnson, C. D. (2004). Acoustic and optical borehole-wall imaging for fractured-rock aquifer studies. *J. Appl. Geophys.* 55 (1-2), 151–159. doi:10.1016/j.jappgeo.2003.06.009

Wu, Y., and Li, P. (2020). The potential of coupled carbon storage and geothermal extraction in a CO2-enhanced geothermal system: a review. *Geotherm. Energy* 8 (1), 19–28. doi:10.1186/s40517-020-00173-w

Xiao, F., Shang, J., and Zhao, Z. (2019). DDA based grouting prediction and linkage between fracture aperture distribution and grouting characteristics. *Comput. Geotech.* 112, 350–369. doi:10.1016/j.compgeo.2019.04.028

Xiao, H., and He, L. (2022). Implementation of manifold coverage for 3D rock fracture network modeling and its application in rock permeability prediction. *Comput. Geotech.* 145, 104702. doi:10.1016/j.compgeo.2022.104702

Xing, Y., Yu, H., Liu, Z., Li, J., Liu, S., Han, S., et al. (2022). Study on chemical genesis of deep geothermal fluid in gaoyang geothermal field. *Front. Earth Sci.* 9, 787222. doi:10.3389/feart.2021.787222

Xu, W., Tang, X., Cheng, L., Dong, Y., Zhang, Y., Ke, T., et al. (2022). Heat flow and thermal source of the xi'an depression, weihe basin, Central China. *Front. Earth Sci.* 9, 819659. doi:10.3389/feart.2021.819659

Younger, P. L., Gluyas, J. G., and Stephens, W. E. (2012). Development of deep geothermal energy resources in the UK. *Proc. Inst. Civ. Eng. Energy* 165 (1), 19–32. doi:10.1680/ener.11.00009

Zhang, B., Wang, S., Kang, F., Wu, Y., Li, Y., Gao, J., et al. (2022). Heat accumulation mechanism of the gaoyang carbonatite geothermal field, hebei province, North China. *Front. Earth Sci.* 10, 858814. doi:10.3389/feart.2022.858814

Zhang, E. Y., Wen, D. G., Wang, G. L., Wang, W. S., Ye, C. M., Li, X. F., et al. (2022). The first power generation test of hot dry rock resources exploration and production demonstration project in the Gonghe Basin, Qinghai Province, China. *China Geol.* 5 (3), 372–382. doi:10.31035/cg2022038

Zhang, L. (2013). Aspects of rock permeability. *Front. Struct. Civ. Eng.* 7, 102–116. doi:10.1007/s11709-013-0201-2

Zhang, Q. H., and Yin, J. M. (2014). Solution of two key issues in arbitrary three-dimensional discrete fracture network flow models. *J. Hydrol.* 514, 281–296. doi:10.1016/j.jhydrol.2014.04.027

Zheng, H., Luo, J., Zhang, Y., Feng, J., Zeng, Y., and Wang, M. (2021). Geological characteristics and distribution of granite geothermal reservoir in southeast coastal areas in China. *Front. Earth Sci.* 9, 683696. doi:10.3389/feart.2021.683696

Zuo, Y., Kong, Y., Jiang, S., Shao, H., Zhu, H., and Yang, M. (2022). Editorial: progress in exploration, development and utilization of geothermal energy. *Front. Earth Sci.* 10, 911376. doi:10.3389/feart.2022.911376